# ULTRASHORT PULSE GENERATION BY

# GAIN SWITCHING

## A MASTER'S THESIS

in

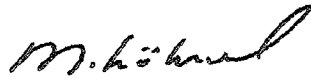Electrical and Electronics Engineering
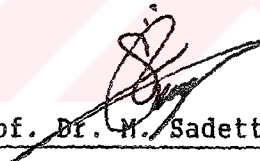University of Gaziantep

By

Muhittin SAYIN

February 1993

Approval of the Graduate School of Natural and Applied Sciences
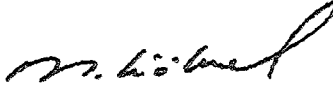
Prof. Dr. Mazhar ÜNSAL
Director

I certify that this thesis satisfies all the requirements as a thesis for the degree of Master of Science.

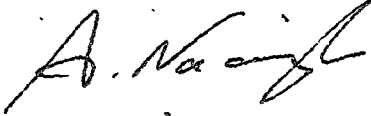Prof. Dr. Muhammet KÖKSAL
Chairman of the Department

I certify that I have read this thesis and that in my opinion it is fully adequate, in scope and quality, as a thesis for the degree of Master of Science.

Assoc. Prof. Dr. M. Sadettin ÖZYAZICI
Supervisor

Examining Committee in Charge:

Prof. Dr. Muhammet KÖKSAL (Chairman)

Assist. Prof. Dr. Arif NACAROĞLU

Assoc. Prof. Dr. M. Sadettin ÖZYAZICI

# ABSTRACT

# ULTRASHORT PULSE GENERATION BY
# GAIN SWITCHING

SAYIN, Muhittin
M. S. in Electrical and Electronics Engineering
Supervisor: Assoc. Prof. Dr. M. Sadettin ÖZYAZICI
February 1993, 99 pages

In this work, ultrashort pulse generation by gain switching in semiconductor lasers is modelled. The model is based on multi-mode rate equations which are numerically solved by using Runge-Kutta-Fehlberg method. Although the standard parameters are taken for 1.3 $\mu$m InGaAsP ridge-wavaguide laser, rate equations are derived in an extended form to be used in the modelling of any semiconductor laser. The important laser diode parameters such as gain compression, Auger recombination and nonradiative recombination are taken into account. In addition, parameters depending on the semiconductor laser dimensions are also included to investigate the effects of laser diode dimensions on the output pulse duration. Short duration optical pulses are generated by applying different electrical signals to the semiconductor laser with the help of this model.

Among the parameters whose effects on the pulse duration are identified, gain compression, laser diode length, gain constant and

Auger recombination are found to be the most important ones.

Comparison of the results with the previous works indicates that single-mode rate equations can not adequately model the generation of ultrashort pulses from laser diodes operating in multi-mode, especially for the lasers having large gain compression or small gain constant.

# ÖZET

## KAZANÇ ANAHTARLAMA YÖNTEMİ İLE

## ÇOK KISA SÜRELİ DARBE ÜRETİMİ

SAYIN, Muhittin
Yüksek Lisans Tezi, Elektrik ve Elektronik
Mühendisliği Bölümü
Tez Yöneticisi: Doç. Dr. M. Sadettin ÖZYAZICI
Şubat 1993, 99 sayfa

Bu çalışmada, yarıiletken lazerlerde kazanç anahtarlama yöntemi ile çok kısa süreli darbe üretimi modellendi. Model, Runge-Kutta-Fehlberg metodu kullanılarak sayısal olarak çözülen çok-modlu değişim denklemleri üzerine kuruldu. Standard parametreler 1.3 $\mu$m InGaAsP tepeli dalga kılavuzlu (ridge-waveguide) lazer için alınmasına rağmen, değişim denklemleri tüm yarıiletken lazerlerin modellenmesinde kullanılabilecek genişletilmiş bir formda elde edildi. Kazanç sıkıştırması, Auger birleşimi ve ısımasız birleşim gibi önemli lazer diyot parametreleri dikkate alındı. Buna ek olarak, lazer diyodu boyutlarının çıkış darbe süresi üzerindeki etkilerini incelemek amacıyla lazer diyodu boyutlarına bağlı olan parametreler de dahil edildi. Bu model yardımıyla yarıiletken lazere çeşitli elektriksel sinyaller uygulanarak kısa süreli optik darbeler üretildi.

Darbe süresini etkileyen parametreler arasında kazanç

sıkıştırması, lazer diyodunun uzunluğu, kazanç sabiti ve Auger birleşiminin en önemlileri olduğu bulundu.

Elde edilen sonuçlar daha önceki çalışmalarla kıyaslandığında, tek-modlu değişim denklemlerinin, özellikle büyük kazanç sıkıştırmasına veya küçük kazanç sabitine sahip çok-modlu çalışan lazer diyotlarından çok kısa süreli darbe üretimini uygun olarak modelleyemeyeceği belirlendi.

Anahtar kelimeler: yarıiletken lazer, kazanç anahtarlaması.

# ACKNOWLEDGEMENTS

# TABLE OF CONTENTS

# LIST OF TABLES

x

# LIST OF FIGURES

# LIST OF SYMBOLS

a(...)     Lattice constant

a          Optical gain coefficient (constant) (in $cm^2$)

$A_{nr}$   Nonradiative recombination coefficient

$\alpha_a$   Absorption loss

$\alpha_c$   Cladding absortion loss

$\alpha_{int}$   Internal loss

$\alpha_m$   Mirror loss

$\alpha_{scat}$   Scattering loss

B          Radiative recombination coefficient

$B_o, B_1$   Radiative recombination coefficients (another form)

$\beta_s$   Spontaneous emission factor (peak of the spontaneous emission spectrum)

c          Velocity of light

$c_o$      Velocity of light in vacuum

C          Auger recombination coefficient

d          Thickness of the active region

D          Normalized waveguide thickness

$D_i$      Normalized Lorentzian lineshape function for gain spectrum

$D_{s_i}$   Normalized Lorentzian lineshape function for spontaneous emission spectrum

$\delta\lambda$   Mode spacing

| | |
|---|---|
| $\Delta\lambda_g$ | FWHM of the gain spectrum |
| $\Delta\lambda_s$ | FWHM of the spontaneous emission spectrum |
| $E_g$ | Band-gap energy |
| $\epsilon_c$ | Gain compression parameter |
| $f_m$ | Modulation frequency |
| $f_r$ | Frequency of relaxation oscillations |
| $g_o$ | Optical gain coefficient (in $cm^3 s^{-1}$) |
| $G_l$ | Linear gain |
| $G_i$ | Modal gain |
| $G_c$ | Gain compression induced gain term |
| $\Gamma$ | (Optical) confinement factor |
| $\Gamma_L$ | Lateral confinement factor |
| $\Gamma_T$ | Transverse confinement factor |
| h | Planck's constant |
| $\eta$ | Refractive index |
| $\eta_a$ | Refractive index of active region |
| $\eta_c$ | Refractive index of cladding region |
| $\eta_g$ | Group refractive index |
| I | Current |
| $I_b$ | DC Bias current |
| $I_{rf}$ | RF current (AC) |
| $I_{th}$ | Threshold current |
| K | Spontaneous emission enhancement factor |
| L | Laser diode length |
| $L_c$ | Composite (external) cavity length |

| | |
|---|---|
| $\lambda$ | Wavelength |
| $\lambda_0$ | Wavelength of the main mode |
| $\lambda_i$ | Wavelength of the i-th mode |
| M | Number of side modes |
| N | Electron density |
| $N_0$ | Electron transparency |
| $\nu$ | Frequency |
| $\nu_g$ | Group velocity of light |
| $P_{o_i}$ | Peak output power of i-th mode |
| $\pi$ | pi number (3.14...) |
| $R_1, R_2$ | Reflectivities of $1^{st}$ and $2^{nd}$ mirror |
| $R_a$ | Auger recombination rate |
| $R_{nr}$ | Nonradiative recombination rate |
| $R_s$ | Spontaneous emission rate |
| $R_{ss}$ | Spontaneous emission rate that couples into the mode |
| $R_{ss_i}$ | Spontaneous emission rate that couples into the mode i |
| S | Photon density |
| $S_i$ | Photon density of i-th mode |
| $S_{i_s}$ | Steady-state photon density of i-th mode |
| t | time |
| $t_d$ | Turn-on delay time |
| T | Round trip time of the laser cavity |
| $\tau_e$ | Effective carrier recombination time |
| $\tau_{nr}$ | Nonradiative recombination lifetime |
| $\tau_n$ | Electron lifetime |

$\tau_p$     Photon lifetime

V        Volume of the active region

w        Width of the active region (width of the ridge
         in RWG laser diode)

# CHAPTER 1

# INTRODUCTION

## 1.1. A BRIEF HISTORY OF SEMICONDUCTOR LASERS

Of all the light sources, the laser was discovered most recently, in 1960; however, it is probably the most important one. There are several ways in which we can classify the different types of lasers. First of all, it can be according to what material or element is responsible for the light amplification; thus, for example, He-Ne laser, the ruby laser, semiconductor lasers, etc.

Since its invention in 1962, the semiconductor injection laser has emerged as an important device in many optoelectronic systems. However, the impact of optoelectronic technology on telecommunications and information systems was not felt until after the 1970s. In 1970, the demonstration of both low loss optical fiber (~20dB/km) waveguide transmission and the room temperature continuous operation of the miniature semiconductor diode laser excited the telecommunications research laboratories worldwide and started a very important chapter in the history of optoelectronics for telecommunications.

Since then, the advances in optoelectronics and lightwave technology have been phenomenal; the practical realization of

optical fiber transmission systems and broadband optical network for telecommunications is making the information age closer to reality. Starting in 1980, the technology of single-mode optical fibers, microelectronics, and semiconductor diode lasers combined is making a truly significant impact on lightwave communication systems. In addition, diode laser based optical information storage and processing systems (compact audio disks, video disks, optical data disks, laser printers, laser bar-code scanners, etc.) also see significant advances after 1980; these are important parts of advanced information systems.

Due to their small size, high efficiency, high speed and ability of being directly modulated, semiconductor lasers become the most important part in the optical communication systems. Diode lasers are the best choice for source applications in optical fiber communication systems, because above specifications fit well with that of optical fibers, small size, lightweight, flexible transmission path with low loss, wide bandwidth and freedom from electromagnetic interference.

The importance of use of InGaAsP as a semiconductor laser material in optical communication systems is the result of minimum attenuation (~0.2 dB/km) and dispersion wavelengths of optical fibers at 1.55 $\mu$m and 1.3 $\mu$m, respectively. Attenuation versus wavelength curve is shown in Figure 1.1 [1]. Quaternary solid solution InGaAsP can easily be lattice matched with InP material in the wavelength range of 0.95-1.7 $\mu$m [2] which covers the lightwave communication wavelengths. This unique property of InGaAsP-InP double heterostructure configuration makes it the best option as a diode laser material for lightwave communication systems. Today,

the use of 1.3 and 1.55 $\mu$m InGaAsP laser diodes in long distance optical communication systems has already reached the commercial stage.
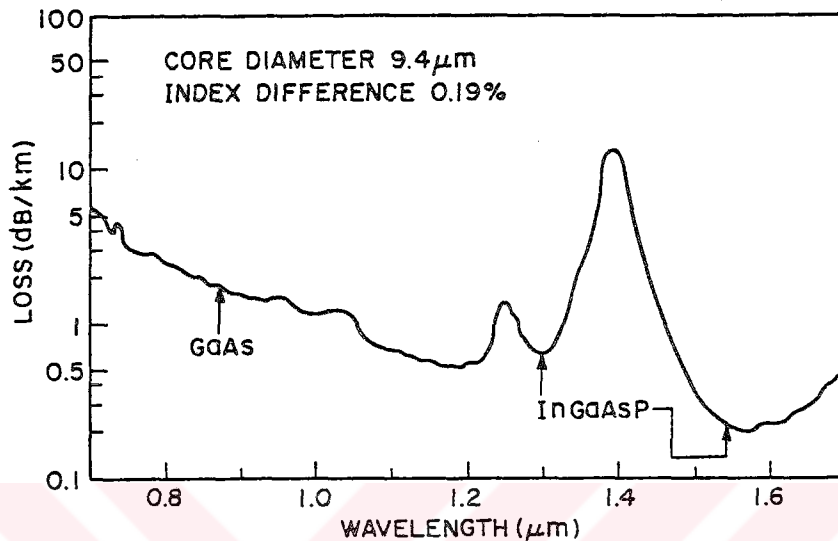


Figure 1.1 Measured loss (attenuation) in a single-mode
silica fiber as a function of wavelength.

## 1.2. OPERATING PRINCIPLES OF SEMICONDUCTOR LASERS

Schematic illustration of a typical double-heterostructure laser is shown in Figure 1.2.

Two things are required to operate a laser: (i) a gain medium that can amplify the electromagnetic radiation propagating inside it and provide the spontaneous emission noise input and (ii) a feedback mechanism that can confine the electromagnetic field through the well-defined optical modes. As the name itself implies, the gain medium for a semiconductor laser consists of a semiconductor material. The optical feedback is obtained using the

3

cleaved facets that form a Fabry-Perot (FP) cavity, and the mode confinement is achieved through dielectric waveguiding. To provide the optical gain, a semiconductor laser needs to be externally pumped, and both electrical and optical pumping techniques have been used for this purpose. A simple, practical, and most commonly used method employs current injection through the use of a forward-biased p-n junction. Such semiconductor lasers are sometimes referred to as injection lasers or laser diodes.
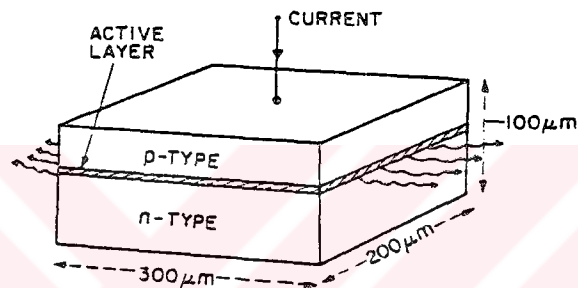


Figure 1.2 Schematic illustration of a double-heterostructure laser with typical physical dimensions.

1.2.1. Lasing and Radiative Recombination Mechanism

The p-n junction is the heart of a semiconductor laser. When it is forward biased by applying an external voltage, the built-in electric field is reduced, making possible diffusion of electrons and holes across the junction. This process corresponds to pumping of electrons from valence band to conduction band. Electrons and holes are present simultaneously in the depletion region and can recombine either radiatively or nonradiatively. Photons of energy $h\nu \cong E_g$ are emitted during radiative recombination as shown in

4

Figure 1.3.b (spontaneous radiative recombination). However, these photons can also be absorbed through a reverse process that generates electron-hole pairs as shown in Figure 1.3.a (absorption). When the external voltage exceeds a critical value, a condition known as population inversion is achieved, in which the rate of photon emission exceeds that of absorption. Spontaneously emitted photons can also stimulate the electrons in the conduction band to recombine radiatively which will give another photon with the same energy ,the same frequency and the same phase as shown in Figure 1.3.c (stimulated recombination). The p-n junction is then able to amplify the electromagnetic radiation through the stimulated emission process. During the each round trip of photons
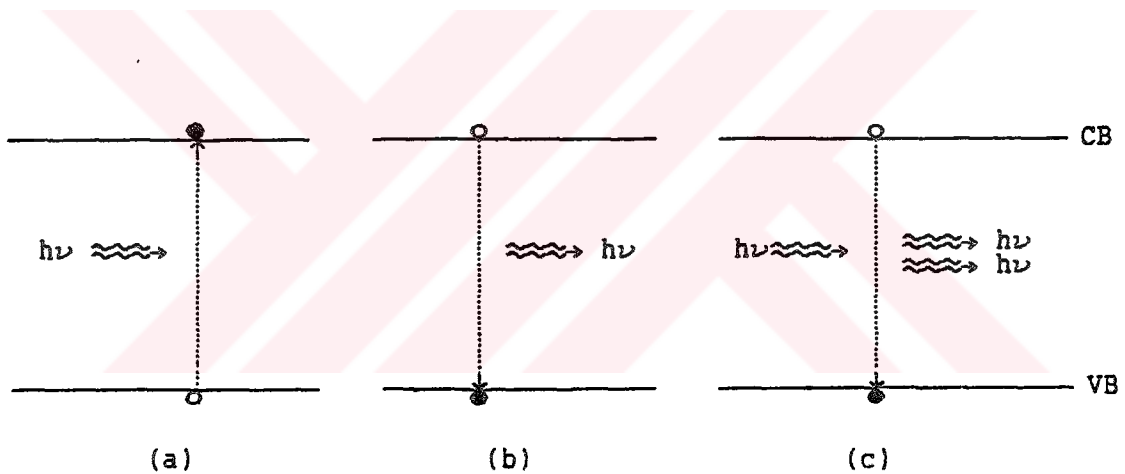


CB-Conduction band, VB-Valence band, o-electron before transition, ⊕-electron after transition.

Figure 1.3 Absorption and emission mechanisms in lasers.
(a) (stimulated) Absorption, (b) spontaneous emission,
(c) stimulated emission.

between the mirrors of the cavity, each photon stimulates one electron to make radiative transition. This process increases rapidly since the round trip time of cavity is in picosecond range, until the energy density in active region reaches a certain value

referred as threshold at which coherent light output from diode facets is emitted. This process is also called as lasing.

Other recombination mechanisms and properties of laser diodes will be investigated in detail through Chapter 3.

## 1.3. MODELLING OF GAIN SWITCHING IN SEMICONDUCTOR LASERS

In this work, a theoretical model of ultrashort pulse generation by gain switching in semiconductor laser diodes is described by a mathematical model based on multi-mode rate equations. Although standard device parameters are taken for 1.3 $\mu$m InGaAsP ridge-waveguide structure laser, the rate equations are derived in an extended form in order to be used in the modelling of any semiconductor laser. The important device parameters such as gain compression, Auger recombination, spontaneous emission, and radiative recombination are also taken into account. Since the diode laser is considered to be operating multi-mode, gain and spontaneous emission terms in rate equations are included in the form of spectrums (wavelength dependent). The reason behind inclusion of gain and spontaneous emission spectrums is that in multi-mode lasers both the gain of each mode and spontaneous emission coupled to each mode will be different.

In addition, parameters depending on the semiconductor laser diode dimensions are included in order to investigate the effect of laser diode dimensions on the pulse duration (FWHM). Although confinement factor, spontaneous emission factor, and photon lifetime are generally considered as constant, they depend on the active region dimensions of the laser diode. Because of this reason

6

their relation with laser dimensions is investigated and these parameters are included in the rate equations in the form that relates them to the laser dimensions. Radiative recombination is taken in a different form than it is generally included in rate equation modelling. This new form is the result of extensive analysis that resulted in carrier density dependent radiative recombination coefficient. This model will be used to generate short optical pulses from semiconductor laser by gain switching. The parameters affecting the pulse duration, gain compression, nonradiative lifetime, radiative recombination, Auger recombination, gain constant, active region thickness, and laser diode length, will be investigated.

# CHAPTER 2

# REVIEW OF ULTRASHORT PULSE GENERATION

# IN SEMICONDUCTOR LASERS

## 2.1. INTRODUCTION

This chapter is intended to provide a review of the basic concepts in ultrashort pulse generation techniques used in semiconductor lasers. There are many methods used for generation of ultrashort pulses from diode lasers. Mode locking, gain switching which is akin to Q-switching in other laser types, injection locking are some well known examples to these techniques. Injection locking technique is rarely used since synchronous operation of two lasers is involved. As it is clear, one of the lasers drive the other by means of it's light output. This configuration requires very careful alignment of the devices, hence is not preferred. Although mode locking and gain switching techniques are quite different from each other, they both employ electrical pumping which is easier than the optical pumping employed in injection locking mechanism. From these facts, it will be better to explain ultrashort pulse generation in semiconductor lasers under the subdivisions of mode locking and gain switching.

## 2.2. REVIEW OF MODE LOCKING IN SEMICONDUCTOR LASERS

Semiconductor lasers are particularly suitable for mode locked operation because of their unique characteristics. Their wide oscillation bandwidth is one of the assets possessed by semiconductor lasers. This enables the generation of mode locked pulses of subpicosecond duration. Other advantages include extremely high efficiency, very small size, and rugged construction. For example, the efficiency of the laser is normally around a few tens percent for CW (continuous wave) operation at room temperature. Decreasing the temperature and allowing pulsed operation lead to efficiencies as high as 60% or more. As for the dimensions of the laser, it would give an idea on the size of typical semiconductor laser if we state that the largest dimension being greater than 400 $\mu$m is uncommon.

The theory of mode locking can be explained as follows; the initial electromagnetic radiation field in the laser cavity is a sum of the oscillating longitudinal modes with random phases and therefore has a noise-like fluctuating spectrum. When the phase difference between the adjacent modes becomes fixed, the fluctuating pattern changes and acquires the characteristics of a well defined pulse.

Mode locking of any laser can be achieved by modulating either loss or the gain of lasers. There are mainly two methods for this purpose, active mode locking and passive mode locking. Other methods, such as, combination of active and passive mode locking, and self locking, are rarely used. The former method requires high technology and careful alignment. Although self locking does not

employ neither an external modulator nor other mode locking element, the main drawback with this technique is the uncontrollable nature of this type of mode locking [3].

## 2.2.1. Passive Mode Locking

Passive mode locking is an effective way of generation of ultrashort pulses. A saturable absorber, whose absorption decreases with higher incident light intensity, is used as mode-locker element. The speed of the saturable absorber affects the mode locking process. In a diode laser, the saturable absorption is presumably from either proton-bombarded region or a dark area of the diode [4]. Passive mode locking by a fast saturable absorber is shown in Figure 2.1. The shaded areas represent excess gain over loss, occurring in every round trip when the pulse saturates the loss due to the absorber whose response time is fast enough to
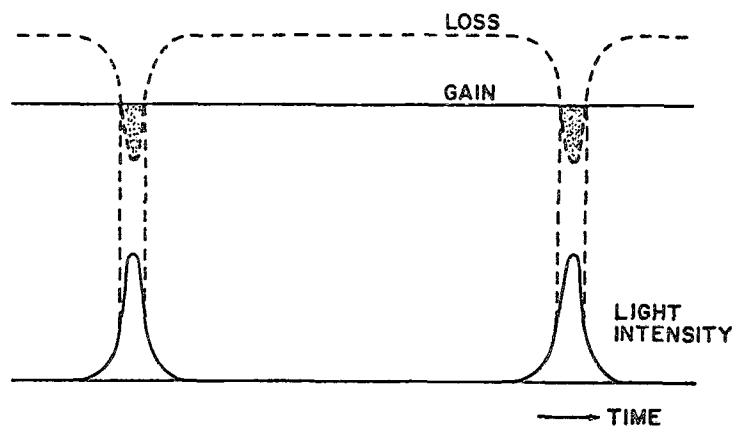
Figure 2.1 Passive mode locking by a fast saturable absorber.

follow the pulse. Figure 2.2 shows the schematic diagram of passive mode locking. Anti reflection coated (AR coated) one end of diode laser allows the light pass through, from the absorber to the external mirror, and when the light intensity inside the cavity reaches very high levels, the absorber saturates and allows the light to go out as an ultrashort pulse. Although this technique gives shorter pulses than active mode locking, since it requires very high epitaxial growth technology to create absorber section, it is rarely used.
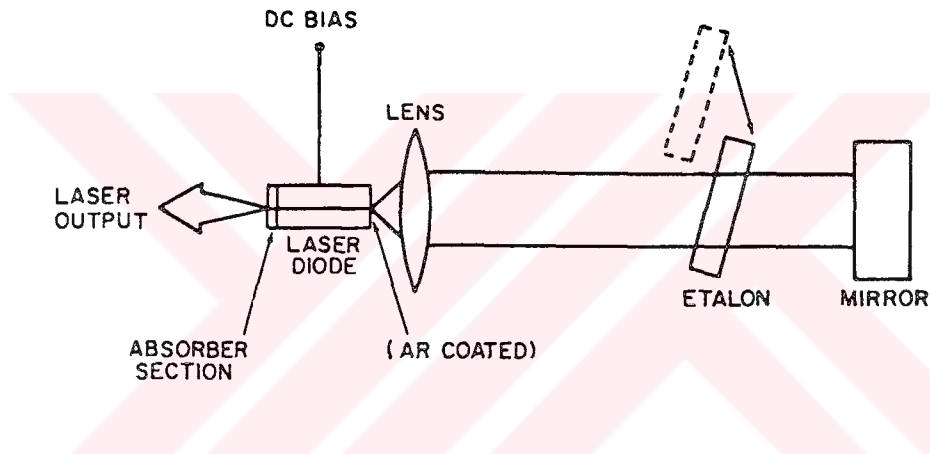


Figure 2.2 Schematic diagram of passive mode locking.

## 2.2.2. Active Mode Locking

Active mode locking is the easiest mode locking technique used in diode lasers since the laser gain can easily be modulated. When the gain of the laser diode in an external cavity is modulated sinusoidally with a frequency equal to the inverse round trip period of the external cavity, the part of the light intensity which passes through the diode at a time when the gain is maximum,

11

will again see maximum gain at subsequent passages. Hence this part
of the intensity will experience rapid growth whereas other parts
will not grow as much because they will pass through the diode at
times of lower gain. Eventually all the energy in the cavity will
be concentrated in the fluctuation pulse which coincides maximum
gain. The partial transmission of this pulse through the one of the
diode facets will constitute the mode-locked laser output which
will be in the form of a train of picosecond pulses with a
repetition rate equal to the inverse round trip time.The process of
formation of ultrashort pulses inside a laser can also be regarded
as a consequence of establishing definite phase relations between
the electric fields of all oscillating longitudinal modes, that is,
mode locking.
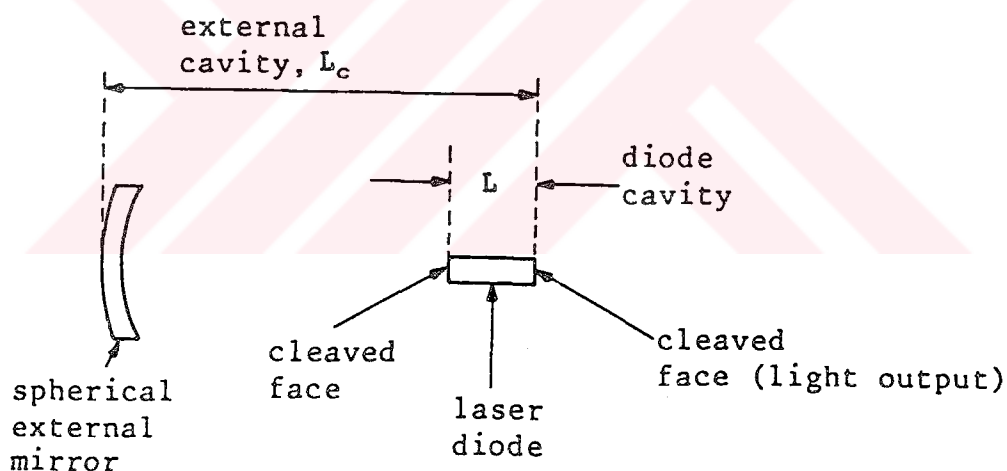
Figure 2.3 The composite semiconductor laser cavity.

Ultrashort pulses by actively mode locking semiconductor
lasers can not be generated with solitary diodes which have typical
lengths of a few hundred microns, since the modulation frequency of
the mode- locker (laser diode itself in the case of semiconductor

lasers) corresponding to these lengths is of the order of a few hundred GHz. Since it is not possible to drive the mode locker (or laser diode ) with the electronic circuits operating at hundred GHz range, and taking into account the frequency response of the device, an external mirror is introduced. A schematic diagram of the composite cavity which is comprised of the external mirror and the laser diode is shown in Figure 2.3. The external cavity is a few tens of centimeters long. The round trip time of the laser cavity in seconds is simply given as

$$T = \frac{2L\eta_a}{c_o} \qquad (2.1)$$

where L is the laser diode length (cm), $\eta_a$ is the active region refractive index, and $c_o$ is the velocity of light in vacuum (cms$^{-1}$). The corresponding drive frequency, $f_m$ (in Hz), is simply equal to the inverse of the round trip time.

From Equation (2.1), a 400 $\mu$m laser with $\eta_a$ being 4, corresponds to a drive frequency of about 188 GHz which is not possible to generate by the electronic circuits available. But in the presence of external cavity, the round trip time becomes

$$T = \frac{2[(L_c - L) + L\eta_a]}{c_o} \qquad (2.2)$$

where $L_c$ is the length of the external cavity (cm). With the same laser used above and 15 cm external cavity length, the drive frequency is found from Equation (2.2) to be about 1 GHz , quite reasonable for the operation.

13

There are basically four reasons why an external cavity is employed for mode locking purposes. These are given in [3,5] as

1) the gain will be able to follow the modulating current, (Otherwise, a modulation current of too high frequency will not be felt effectively by the active medium due to finite lifetime of the injection carriers.)

2) the frequency of modulation of the injected current will be within the practically realizable limits (as explained above),

3) the number of modes oscillating will be increased, and

4) the threshold of the laser diode will be reduced (since it is inversely proportional to the cavity length).

The external cavity required for mode locking can take a number of forms [5], including a spherical mirror,lenses and mirrors, a SELFOC lens or a length of optical fibre.
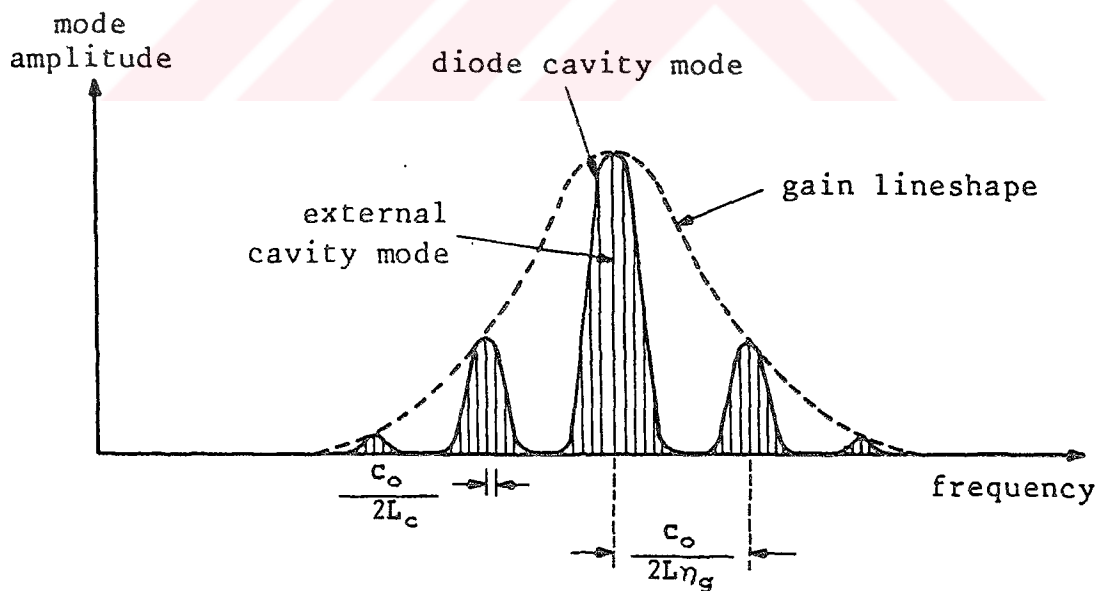


Figure 2.4 Longitudinal modes of the composite cavity.

14

The composite cavity has two kinds of axial (longitudinal) modes: those belonging to the diode cavity, and those belonging to the external cavity. Figure 2.4 shows both types of longitudinal modes of the composite cavity. The width of the resonance peak of the Fabry-Perot consisting of the low reflectivity laser diode mirrors (typically 32%) is much broader than the width of the external resonator formed by 100% reflecting mirror and one of the laser diode facets. Since the frequency spacing of the modes of the external cavity is much smaller than the frequency spacing of the diode cavity modes, the amplitude of the axial modes of the external cavity will be modulated by the axial modes of the diode cavity. When modulation applied to the composite cavity, diode cavity modes can not usually be phase locked. Hence, only those external cavity modes which are situated within the frequency spread of a single diode cavity mode can be successfully mode locked. If more than one cavity mode is excited (as is usually the case) then the phases of the external cavity modes which are within the frequency spread of one diode cavity mode will not have a fixed relationship with the phases of the external cavity modes within the frequency spread of an adjacent diode cavity mode. This means that, the oscillating external cavity modes will be locked in groups and complete mode locking of all oscillating longitudinal modes will not occur. The pulses produced will not be transform limited (minimum duration) and will contain temporal substructure on the pulse envelope. For successful mode locking of laser diodes, the oscillation spectrum should be restricted to a single longitudinal mode or the Fabry-Perot resonator resulting from the partially reflecting laser diode mirrors should be removed. Simply,

15

after removing one of the laser diode mirrors (by AR coating) which faces the external mirror, the longitudinal modes of the diode cavity will take the form shown in Figure 2.5, where the amplitudes of the external cavity modes will be determined only by the gain lineshape. The schemes which used in practice to modify the
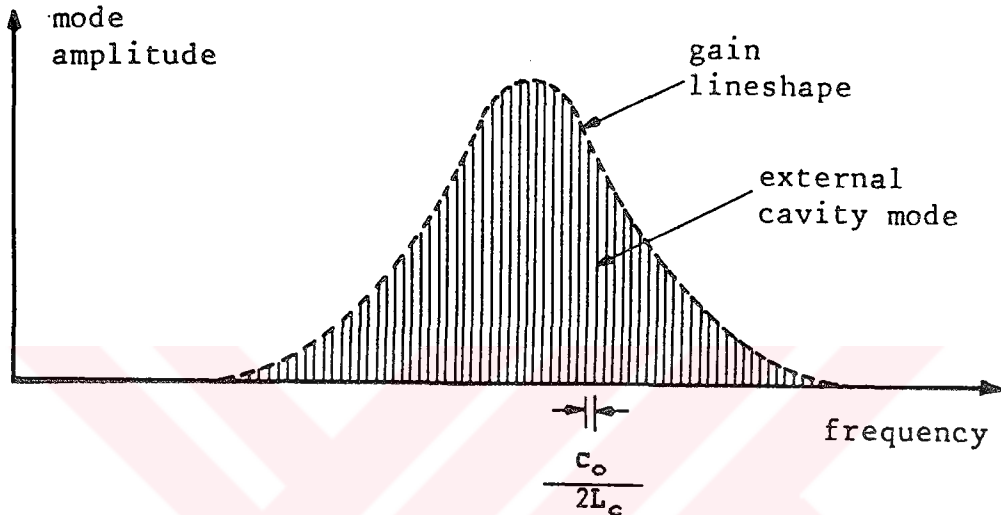
Figure 2.5 Longitudinal modes of the composite cavity with one facet of the laser diode AR coated.

oscillation spectrum of the laser diodes can be summarized as [3,5]

1) an intracavity Fabry-Perot etalon acting as an optical filter which should have a bandwidth large enough to allow only one diode cavity mode through,

2) a reflecting diffraction grating can be used instead of a plane mirror and an etalon,

3) tilting the stripe of the laser diode or polishing the facet of the laser diode at the Brewster angle can suppress the total internal reflections at the diode facet and hence remove all the diode cavity modes,

16

4) anti-reflection (AR) coating one of the laser diode facet will remove all the diode cavity modes.

An actively mode locked semiconductor injection laser configuration is given in Figure 2.6.

As explained before, active mode locking of laser diodes is achieved by exciting the laser diode simultaneously with DC and RF current at a frequency equal to the inverse round trip period. Mode
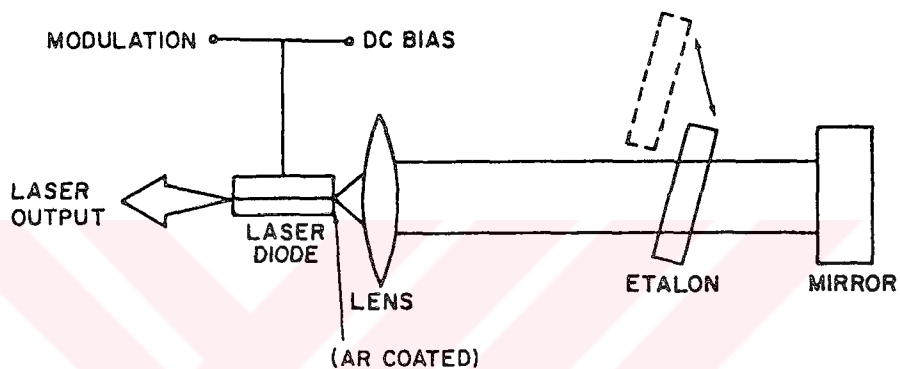


Figure 2.6 Schematic diagram of active mode locking.

locking can also be performed by modulating the injection current of the laser diode at a frequency which is integer multiple of the fundamental frequency corresponding to the external cavity length. This technique is known as harmonic mode locking [6] and used to generate short duration mode locked pulses at very high repetition rates [7]. The DC current bias is usually greater than the threshold current [8], although mode locking has also been achieved by using a bias which is considerably less than the threshold current [9], or exactly equal to it. For gain modulation in active mode locking, repetitive electrical pulses instead of sinusoidal RF modulation can also be used [9]; non-sinusoidal modulation has the

advantage of biasing the laser significantly above threshold thus providing higher output powers. Also, more stable mode locking has been reported with this type of modulation. A comparison of the results of the models, detailed analysis of active mode locking in semiconductor lasers and optimum conditions have been extensively explained in [10].

## 2.3. REVIEW OF GAIN SWITCHING IN SEMICONDUCTOR LASERS

Ultrashort pulses generated by semiconductor lasers can find important applications in high bit-rate optical fibre communication systems. The simplest and most versatile scheme for producing short pulses from diode lasers without using any external cavity is known as gain switching; in which the gain is modulated with electrical pulses.

The mechanism of gain switching can be explained as follows. The optical output from the laser diode does not reach steady-state immediately if an electrical pulse greater than the threshold value is applied to the laser diode. The diode laser exhibits a transient response in the form of damped oscillations (relaxation oscillations) and eventually reaches to steady-state as shown in Figure 2.7. If the duration of the applied electric injection pulse is short, the threshold is overcome momentarily and the output is a single pulse which is essentially the first peak of the relaxation oscillations. Each light pulse generated then corresponds to one of the electric pulses, that is, for periodic injection pulses, the repetition rate of the optical pulses at the output is the same as the frequency of the applied modulation current. The duration of
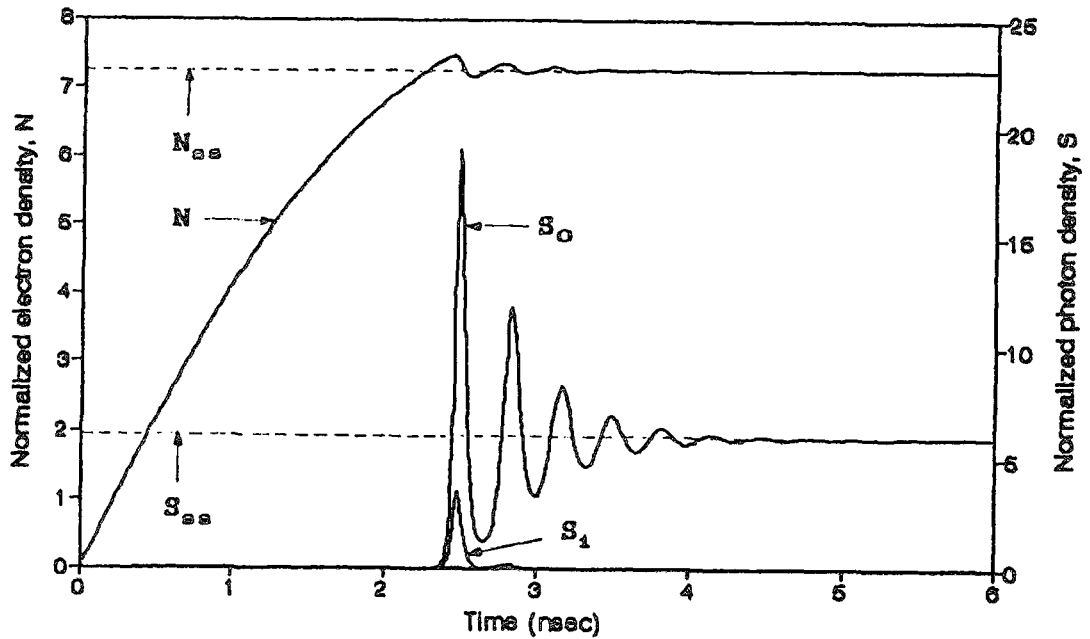
Figure 2.7 Transient response of a gain switched laser diode (relaxation oscillations).

the output pulse (FWHM) depends on the magnitude and to a certain extend on the duration of the driving electrical pulse, as well as to the length of the cavity. High amplitude driving pulses with a short duration, low threshold and short cavity length produce a short optical pulse. Some other factors affecting the output pulse duration will be investigated in this thesis.

Gain switching is similar to Q-switching, but because of the short photon lifetime associated with semiconductor lasers, the pulse widths are only a few tens of picoseconds in duration. Gain switching can be affected by applying a suitable modulation current waveform on the DC bias current. In practice, the gain can either be directly modulated by large RF sinusoidal (or half sinusoidal) current [11,12] or triggered by short electrical pulses of large amplitude from comb generator [13,14].

19

The experimental feasibility of generating 20-30 psec pulses by gain switching in directly modulated AlGaAs and InGaAsP lasers is extensively studied. The minimum duration pulses have reported to be 11-13 psec [15,16] with InGaAsP lasers. The highest repetition rate of 11.2 GHz with pulses of 25 psec from a gain switched short cavity InGaAsP laser biased above threshold has been reported [17]. The generation of high peak power of 1.2 W with 28 psec pulse duration at 210 MHz repetition rate from an InGaAsP laser operating at 1.3 $\mu$m has also been demonstrated. Optical pulses with bandwidth-limited character has been produced from the gain switching of a distributed feedback InGaAsP laser [18]. One of the disadvantages of gain switching is that if the DC bias is below threshold, lasing may cease between pulses so that optical coherence between pulses is lost.

## 2.3.1. Effect of DC Bias Current on the FWHM of Pulses

Gain switching of semiconductor lasers can be performed at any (even negative) DC bias current. It has been shown theoretically that shorter optical pulse durations can be obtained for higher values of DC bias [19]. Calculations performed by Ito et al. [20] and Van der Ziel et al. [21] indicate a similar conclusion. Supporting experimental observations are also reported in [12,13,21]. On the contrary, calculations based on a similar theoretical model used in [19,20] indicate that the pulse duration decreases with decreasing DC bias current [22]. The theoretical result obtained in [22] has been supported by the experiments performed in [18,22,23]. A more extensive single-mode rate equation

20

analysis performed by Özyazıcı et al [24] indicate the same trend of DC behavior of laser diodes as indicated in [18,22]. In another experimental paper [14], it was found that the pulses are broadened if the DC bias is too large. It has been experimentally demonstrated that there is an optimum DC bias current near the DC threshold for which the pulse duration is minimized [16,24]. It has been also indicated [16,24] that the pulse broadens if it is biased below this optimum current level. Auger recombination is given to be responsible for the pulse broadening for higher values of DC current [5]. The experimental results of [16,24] show that the pulse width becomes insensitive to the DC bias current if laser diode is biased a few milliamperes above its threshold current. So, there is a contradiction of the dependence of the pulse duration on the applied DC bias current.This contradiction is yet to be resolved.

## 2.3.2. Effect of Modulation Frequency on the FWHM of Pulses

A wide range of modulation frequencies can be used in the gain switching technique; unlike active mode locking, no particular modulation frequency is required. It has been shown [19] that multiple pulses due to relaxation oscillations will occur if the modulation frequency is too low. By increasing the modulation frequency the number of relaxation spikes appearing at the output decreases, until eventually single pulse per modulation period is achieved. This dependence on the modulation frequency has been experimentally observed [20]. But, the modulation frequency cannot be increased beyond a certain value known as the cut-off frequency

beyond which only spontaneous emission due to DC bias excitation was observed [20]. It has been found that the value of the cut-off frequency depends mainly on the electron lifetime $\tau_n$ and to a lesser extent on the DC bias and modulation current amplitudes. Since $\tau_n$ is of the order of nanoseconds, the electrons cannot respond to modulation frequencies above several hundred MHz, so oscillation ceases. However, it has been indicated [17] that the high frequency gain switching characteristics of semiconductor lasers are directly related to the high-speed modulation response of the laser. This modulation depends mainly on the electron lifetime $\tau_n$, the photon lifetime $\tau_p$ and the DC bias current. So the modulation response of the laser diode can be increased by decreasing the photon lifetime or increasing the DC bias current. This way, gain switching at high frequency is possible. This explains the lack of cut-off in gain switching experiments performed beyond 1 GHz in [12,17,19]. It has been shown theoretically [20] that the pulse width increases if the modulation frequency increases. On the contrary, theoretical and the experimental results given in [12,18,22] indicate that the pulse width decreases if the frequency of the modulation is increased. Although, there is no difference between the theoretical models used in the calculations, the results are completely different. The common feature of the models is that the RF current is used to modulate the gain of the laser diode. This means that the width of the sine wave gets shorter if the frequency of the RF current increases. Since the laser diode is gain switched with shorter pulses, the pulse width obtained should be shorter as well. Hence, the results given in [18,22] represents the true behaviour of the

22

gain switched laser diode.

### 2.3.3. Effect of Photon Lifetime on the FWHM of pulses

Decreasing the photon lifetime can also produce shorter pulses. It has been experimentally and theoretically demonstrated that the pulse width decreases if the photon lifetime is decreased [20,21,25]. Recent calculations based on the multi mode rate equations reveal that optical pulses as short as 10 psec are possible with short cavity lasers with reflective coatings [26].

### 2.3.4. Effect of RF Current on the FWHM of Pulses

The effect of the amplitude of the modulation current has also been observed, keeping the DC bias current and the frequency of modulation constant [20,24]. Any excess increase in the amplitude of the RF current gave rise to multiple pulses per modulation period in the output. In addition, increasing the modulation amplitude causes a decrease in the DC threshold [24,25,27]. The theoretical and experimental results given in [12,20,21,24] indicate that the pulse width decreases if the amplitude of the RF modulation current increases. In addition, an optimum RF current at which the pulse width is minimized is given in [24].But the conclusion reached in [25] does not support the dependence of the pulse width on the amplitude RF current. It has been found [25] that the pulse width produced are fairly insensitive to the RF drive level. However, no theoretical calculations have been performed in [25] to support their

23

conclusion.

The dependence of the peak power of the pulses obtained from the gain switched laser diode on the DC and RF current has been depicted in [12,16,20,22]. It has been found [12,16,20] that the peak power decreases if the DC bias current is decreased. On the other hand, it has been demonstrated [22] that the peak power increases if the DC bias current is decreased well below the threshold current. The results given in [12,20] indicate that the peak power also decreases with decreasing RF modulation current. The results given in [20,22] agree that the peak power decreases if the modulation frequency is increased at fixed DC bias current and RF current. Although increasing the frequency of modulation decreases the pulse width, this results in less peak power.

In the majority of gain switching experiments, sinusoidal RF modulation is employed. Direct comparison of the pulse widths obtained from the RF current modulation and electrical pulse modulation of the gain switched laser diode is given [21]. It has been found that electrical pulse excitation produces shorter pulses. It has been explained [21] that shorter pulse width is due to the more rapid time dependent increase in the gain which results in a higher level of excitation and hence stimulated emission. It has been indicated [16,21] that the pulse width is limited by the dynamic properties of the semiconductor lasers and not by the duration of the electrical pulses used in the gain switching experiments.

Theoretical treatment of the gain switching process in semiconductor lasers is based on the rate equations. Rate equations can be single or multi-mode depending on whether the semiconductor

24

laser is operating in single or multi-mode. Even though the diode laser is operating multi-mode, using a single-mode rate equation model gives sufficiently accurate results if the oscillating modes are not coupled [20]. This seems to be a valid assumption, since in gain switched operation, proper mode locking does not occur [5]. Rate equations will contain some extra terms depending on the type of semiconductor laser used in the gain switching. Auger recombination, nonradiative recombination (recombination through traps) and gain compression or gain saturation due to lateral carrier diffusion are important processes in InGaAsP based semiconductor lasers. Therefore, these processes should be taken into account in the rate equation model of this type of gain switched semiconductor laser.

# CHAPTER 3

# RATE EQUATIONS MODEL OF

# GAIN SWITCHED LASER DIODE

## 3.1. INTRODUCTION

Rate equations for a laser diode can simply be defined as a pair of equations that relates the input to the electron density injected into active region and photon density emitted from laser diode with respect to time. Input can either be electrical or optical in semiconductor lasers. For single-mode operation, two equations for electron and photon densities are enough to explain laser dynamics. However, in the case of multi-mode operation, an equation for electron density and a number of equations for each longitudinal mode must be included. In addition, gain spectrum and spontaneous emission spectrum must also be included in multi-mode rate equations since each mode experiences different gain (or loss), and contribution from spontaneous emission to each mode will be different.

Rate equations are solved to predict the laser's static, spectral and dynamic response for a given input. Since the invention of laser in late 1950s, scientist have tried to simulate the laser action by rate equations based on the Einstein's

explanations on the electronic transitions between atomic levels. These equations first used in 1960, just after the invention of the laser, and have been used extensively for semiconductor lasers after 1964, two years later than the first semiconductor laser operation. Since then, there have been many changes (additions) in rate equations for better explanation of laser action to get similar results as obtained from experiments. The main reason behind so much attention is that; simulating the laser action by proper formulas can be used both to obtain optimum operating conditions and to determine the required input for a needed output (especially after the use of very fast computers in numerical analysis). For diode lasers, these equations and modeling have been investigated widely especially after the invention of low loss fiber used in the lightwave communication systems , since the use of laser diodes as a source seemed to be the best candidate for these systems. The source spectral width and FWHM of pulses from diode laser are the key parameters for determination of, pulse broadening, bandwidth, and maximum repeaterless distance achievable for optical fibre communication systems. Generation of ultrashort pulses with a minimum FWHM have been extensively studied in semiconductor lasers operating at 1.3 and 1.55 $\mu$m, since these wavelengths are the minimum dispersion and minimum loss wavelengths for fiber-optic communication systems, respectively. The important point is that the rate equation model must explain the laser action so well that, the experimental and theoretical results would be nearly the same. This fact explains why so much work has been done on rate equation model and modifications made through it.

For a better understanding of ultrashort pulse generation,

some basic mechanisms in semiconductor lasers must be explained before giving the complete rate equations. These are gain, stimulated emission, spontaneous emission, nonradiative recombination, confinement mechanism , modes, losses and photon lifetime.

## 3.2. GAIN AND STIMULATED EMISSION

Laser gain due to stimulated emission is explained under the subdivisions of linear gain, gain lineshape and gain compression (or gain saturation).

### 3.2.1. Linear Gain

In basic approach, a generalization is made on the Einstein's coefficients which relate the rate of spontaneous emission and stimulated emission to the net gain or absorption coefficient. A shortcoming of this approach is that; it provides only the small-signal gain and so gain saturation effects cannot be treated. By this approach, after the observation of numerically calculated gain at the lasing frequency, variation of gain can be assumed to be linear with injected carrier density N ($cm^{-3}$) for all values of input. Carrier density dependent linear gain ($cm^{-1}$) can be approximated by [1]

$$G_L(N) = a(N - N_o) \tag{3.1}$$

where a is the gain coefficient ($cm^2$) and $N_o$ is the carrier density

required to achieve transparency (corresponding to the onset of population inversion). Linear gain can also be written as $(s^{-1})$

$$G_l(N) = g_o(N - N_o) \qquad (3.2)$$

where the gain coefficient $g_o$ $(cm^3 s^{-1})$ is related to a in Equation (3.1) as

$$g_o = a\nu_g \qquad (3.3)$$

$$\nu_g = \frac{c_o}{\eta_g} \qquad (3.4)$$

where $\nu_g$ is the group velocity of light in active region $(cms^{-1})$, $\eta_g$ is the group refractive index ($^\sim$4 for InGaAsP) and $c_o$ is the velocity of light in vacuum.

## 3.2.2. Gain Spectrum

For semiconductor lasers operating in multi-mode gain spectrum must also be taken into account. In semiconductor lasers the gain spectrum is homogeneously broadened since the intraband carrier scattering time is extremely short ($^\sim$100 fsec) so that all stimulated recombination process can be assumed to occur between the minimum of conduction band and maximum of valence band. Homogeneously broadened lasers have Lorentzian lineshape as shown in Figure 3.1. The normalized Lorentzian lineshape function is given by [28,29]

$$D_i(\lambda) = \cfrac{1}{1 + \left[\cfrac{2(\lambda_o - \lambda_i)}{\Delta\lambda_g}\right]^2} \qquad (3.5)$$

where $\lambda_o$ is the wavelength of the main mode (nm), $\lambda_i$ is the i-th mode wavelength, and $\Delta\lambda_g$ is the FWHM of the gain spectrum (nm). For
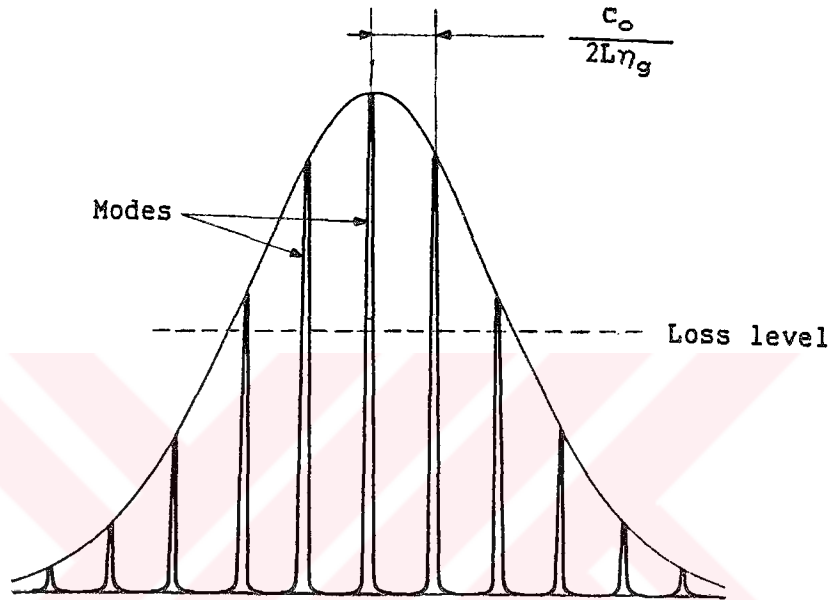


Figure 3.1 Gain spectrum of the laser diode in the form of Lorentzian lineshape function.

the symmetrical placement of longitudinal modes, the distance between the modes is constant and given by

$$\delta\lambda = \frac{\lambda_o^2}{2L\eta_g} \qquad (3.6)$$

$$\delta\lambda = |\lambda_o - \lambda_1| = |\lambda_1 - \lambda_2|$$

$$= |\lambda_o - \lambda_{-1}| = |\lambda_{-1} - \lambda_{-2}| \qquad (3.7)$$

30

where $\delta\lambda$ is referred as longitudinal mode spacing (nm), $\lambda_1$ and $\lambda_2$ are the wavelengths of 1st and 2nd modes placed at the right of the main mode, $\lambda_{-1}$ and $\lambda_{-2}$ are the wavelengths of the modes placed at the left of the main mode, respectively. The distance of i-th mode from the central mode can be written from Equation (3.7) as

$$\lambda_0 - \lambda_i = i\delta\lambda \qquad (3.8)$$

Equation (3.8) can be used to simplify the normalized Lorentzian lineshape function given by Equation (3.5). So, the normalized Lorentzian lineshape function will be

$$D_i(\lambda) = \frac{1}{1 + \left[\dfrac{2i\delta\lambda}{\Delta\lambda_g}\right]^2} \qquad (3.9)$$

Since modes are symmetrically placed around main mode as shown in Figure 3.1, Equation (3.9) gives same $D_i(\lambda)$ values for $\mp$ i-th modes.

By combining the normalized Lorentzian lineshape function $D_i(\lambda)$ with linear gain $G_l(N)$, modal gain (without gain compression term) can be written as [30]

$$G_i(N,\lambda) = g_0(D_i N - N_0) \qquad (3.10)$$

### 3.2.3. Gain Compression

Gain compression (also referred as gain saturation) is an important phenomena for semiconductor lasers, especially for InGaAsP which shows unignorable gain compression. Gain saturation is caused by several mechanisms such as spatial hole burning and lateral carrier diffusion, spatial hole burning, and other nonlinearities. All these mechanisms are known to enhance multi-mode oscillation and their effects can be stressed by a constant named as gain compression parameter ($\in_c$).

Spatial hole burning (in both lateral and longitudinal directions) is a result of standing-wave nature of the optical field in the cavity and is known to lead multi-mode oscillation. However, its relative importance depends on the carrier diffusion whose effectiveness decreases with an increase in the laser power since the stimulated recombination time becomes much shorter relative to the carrier diffusion time. As a result, side mode power starts to increase when the main mode power exceeds some critical value. Simply, the spatial distribution of the population inversion determines the gain of different cavity modes and, therefore, which mode or modes will lase.

Spectral hole burning is related to the broadening mechanism of the gain profile. At high laser powers the stimulated recombination time becomes small enough (~1 psec) that the peak gain decreases because of partial spectral hole burning. Consequently, other longitudinal modes start to grow, and the range of single mode operation is inherently limited.

The most important of these gain saturation mechanisms are

lateral spatial hole burning and spectral hole burning. Lateral spatial hole burning is usually neglected in high-speed InGaAsP lasers in preference to the more dominant effect of spectral hole burning of which relative importance increases as almost square of the cavity width [30].

For simplicity, all these effects are included in one parameter $\in_c$, which takes values between $3\times10^{-17}$ and $6.7\times10^{-17}$cm$^3$ for InGaAsP lasers [31-34]. Effect of gain compression in laser action can be included in the following form [35]

$$G_c(S_i) = \frac{1}{1 + \in_c\sum S_i} \tag{3.11}$$

where $S_i$ is the i-th mode photon density in cm$^{-3}$, and the term $\sum S_i$ denotes the sum of photon densities of all modes. In some works, for example in [36], Equation (3.11) is taken as

$$G_c(S_i) = 1 - \in_c\sum S_i \tag{3.12}$$

which is the first term of the Taylor series expansion of the equation (3.11) and can be used in small-signal analysis since the sum of the photon densities will be small.

Inclusion of gain compression term in modal gain leads the complete gain term as

$$G_i(N,\lambda,S_i) = G_i(N,\lambda)G_c(S_i) \tag{3.13}$$

By removing the independent variables for simplicity and putting

equalities of all the terms included at the right hand side,
complete modal gain as a function of electron density, photon
density, and wavelength can be rewritten using Equation (3.10) and
Equation (3.11) as

$$G_i = \frac{g_o}{1 + \epsilon_c \Sigma\, S_i} \left\{ \frac{1}{1 + \left[\dfrac{2i\delta\lambda}{\Delta\lambda_g}\right]^2}\, N - N_o \right\} \qquad (3.14)$$

## 3.3. RADIATIVE SPONTANEOUS EMISSION

Spontaneous emission plays an important role especially
before lasing threshold is reached. Its inclusion in rate equations
is in the form of total spontaneous emission rate given by
$(cm^{-3}s^{-1})$ [1]

$$R_s = BN^2 \qquad (3.15)$$

where B is the radiative recombination coefficient which is
calculated to be in the range of $0.7\text{-}1.5\times10^{-10}cm^3s^{-1}$ for 1.3 $\mu m$
InGaAsP lasers [1].

However, it has been calculated that spontaneous emission
occurs in a certain wavelength range and has a spectrum like gain
lineshape which is Lorentzian. Another important fact is that peak
of the spontaneous emission spectrum changes with injected carrier
density N. An extensive analysis of calculated spontaneous emission

spectrum for different carrier injection levels in 1.3 $\mu$m InGaAsP has led to a carrier density dependent radiative recombination which may be written as [1]

$$B(N) = B_O - B_1N \qquad (3.16)$$

where $B_O$ and $B_O$ to $B_1$ ratio is calculated to be in the range of $0.5-0.7\times10^{-10}$cm$^3$s$^{-1}$ and $1.7-2.2\times10^{-19}$, respectively [1]. Since Equation (3.16) is more accurate than Equation (3.15), Equation (3.16) will be used in this work. With Equation (3.16), spontaneous emission rate given by Equation (3.15) now becomes

$$R_s = (B_O - B_1N)N^2 \qquad (3.17)$$

### 3.3.1. Spontaneous Emission into the Modes

Although Equation (3.17) gives the total spontaneous emission rate, all of this rate does not goes into the lasing mode or modes. It is assumed that a fraction $\beta_s$ of spontaneously emitted photons goes into the lasing mode. So, the part of the spontaneous emission that couples to mode can be written as

$$R_{ss} = R_S\beta_s \qquad (3.18)$$

$\beta_s$ is also called as spontaneous emission factor, and in practice, treated as a fitting parameter. Its typical value for index-guided InGaAsP lasers is in the range of $10^{-4}-10^{-5}$.

35

An alternative and more accurate way of expressing $\beta_s$ in terms of laser parameters is [1,28]

$$\beta_s = \frac{K\Gamma\lambda_o^4}{8\pi^2\eta_a^2\eta_g\Delta\lambda_s V} \qquad (3.19)$$

where K is the enhancement factor and is equal to 1 for index-guided lasers but greater than one for gain-guided lasers. $\Gamma$ is the optical confinement factor which denotes the fraction of optical power confined to the lasing ,of which numerical value changes between 0.2-0.4 for Fabry-Perot lasers. $\eta_a$ is the effective mode index , or active region refractive index and is typically 3.4 for 1.3 $\mu$m InGaAsP lasers. $\Delta\lambda_s$ is the FWHM of the spontaneous emission spectrum (typically 50-100 nm) and is bigger than the width of the gain spectrum $\Delta\lambda_g$. V stands for the active region volume which is

$$V = Lwd \qquad (3.20)$$

L, w, d are laser length, active region width and active region thickness, respectively.

In the case of multi-mode operation, spontaneous emission spectrum must also be included since the contribution from spontaneous emission to different modes will be different. As mentioned above, this spectrum is in the form of gain spectrum and is Lorentzian. Normalized Lorentzian lineshape function for spontaneous emission spectrum can be written as

$$D_{s_i}(\lambda) = \frac{1}{1 + \left[\dfrac{2(\lambda_o - \lambda_i)}{\Delta\lambda_s}\right]^2} \qquad (3.21)$$

as it is clear this equation is same as Equation (3.5) except the term $\Delta\lambda_g$ is replaced with $\Delta\lambda_s$. Using the same simplifications derived through Equation (3.6) to Equation (3.8) this spectrum reduces to a form similar to Equation (3.9) as

$$D_{s_i}(\lambda) = \frac{1}{1 + \left[\dfrac{2i\delta\lambda}{\Delta\lambda_s}\right]^2} \qquad (3.22)$$

By using this equation and Equation (3.19) which is the peak of the spontaneous emission factor, Equation (3.18) becomes

$$R_{ss_i} = R_s\beta_s D_{s_i} \qquad (3.23)$$

where $R_{ss_i}$ is spontaneous emission that coupled to i-th mode. Equation (3.23) can be rewritten in the expanded form as

$$R_{ss_i} = (B_o - B_1 N)N^2 \frac{K\Gamma\lambda_o^4}{8\pi^2\eta_a^2\eta_g\Delta\lambda_s V} \frac{1}{1 + \left[\dfrac{2i\delta\lambda}{\Delta\lambda_s}\right]^2} \qquad (3.24)$$

## 3.4. NONRADIATIVE RECOMBINATION

An electron-hole pair can also recombine nonradiatively. In this process photon emission does not take place, instead energy

37

goes into lattice phonons. In many semiconductors, for example, pure germanium or silicon, the nonradiative recombination dominates the radiative recombination. Since this type of recombination takes a part of the input energy, it increases the threshold current. Moreover, since number of phonons created will reach tremendous amount, device heat will get bigger and operating lifetime of the laser diode will be reduced as it was in the case of the first generation semiconductor lasers.

The nonradiative recombination process can be divided into two main groups, Auger recombination and defect and surface recombination.

### 3.4.1. Auger Recombination

It is accepted that Auger recombination can be a major nonradiative recombination mechanism in narrow-gap semiconductors. So much attention to this type of recombination has been in connection with the observed greater higher temperature dependence of threshold of long-wavelength InGaAsP lasers compared to short-wavelength AlGaAs lasers. It is generally believed that Auger recombination plays a significant role in determining the observed high temperature sensitivity of threshold current of InGaAsP lasers emitting near 1.3 and 1.55 $\mu$m.

There are several types of Auger recombination process. The three major types are band-to-band process, phonon-assisted Auger process, and trap-assisted processes. Phonon-assisted process dominates at high band-gap materials and therefore can be neglected in long-wavelength operation in which band-to-band process

38

dominates. Trap-assisted process is very important only in heavily doped n or p-type semiconductors with a high concentration of traps below and the above the Fermi level, respectively. So, band-to-band process is very important in intrinsic long-wavelength InGaAsP lasers.

As in all other types of Auger processes, band-to-band Auger process involves three particles, either two electrons and one hole, or two holes and one electron. The band-to-band Auger recombination for a direct band semiconductor with parabolic valence and conduction bands is shown in Figure 3.2. The two electrons and one hole (eeh) process is shown in Figure 3.2.a. Here



(a)                              (b)

E-Energy, k-wavevector
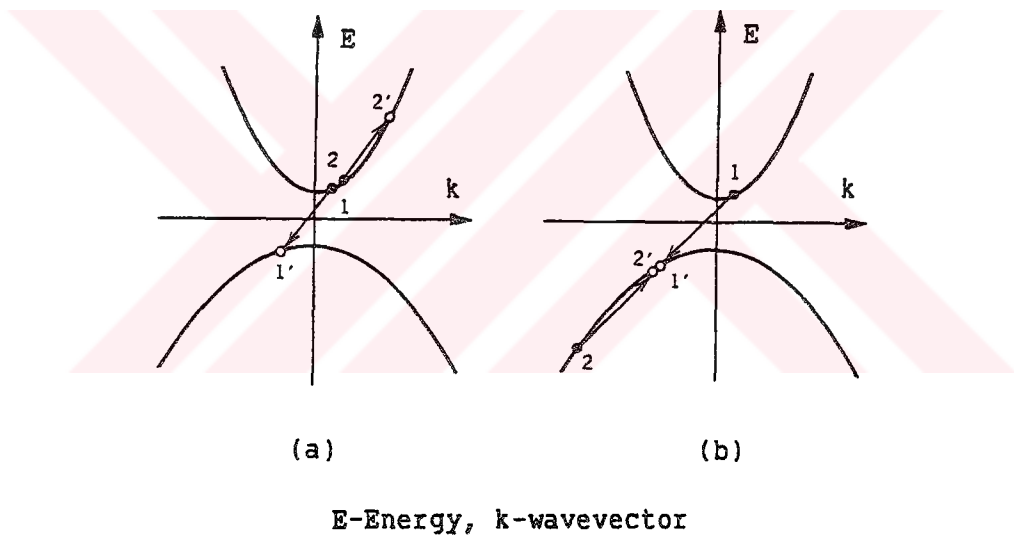
Figure 3.2 Band-to-band Auger recombination in a direct gap semiconductor with parabolic valence and conduction bands; (a) eeh process and (b) ehh process.

electron 1 in the conduction band makes a transition to an empty state 1' in the valence band. The energy of electron-hole pair is then transferred to the nearby electron 2, which rises high in the conduction band to the state 2'. The excited electron now loses its kinetic energy as lattice phonons and returns to the thermal

39

equilibrium. Figure 3.2.b shows the similar process occurred by means of two holes and one electron (ehh).

Since the active region of the InGaAsP laser is nominally undoped, under high injection the Auger rate $R_a$ $(cm^{-3}s^{-1})$ varies approximately as [1]

$$R_a = CN^3 \qquad\qquad (3.25)$$

where C is the Auger recombination coefficient $(cm^6s^{-1})$. Measured values of C lies in the range $1-7.5\times10^{-29}cm^6s^{-1}$ for InGaAsP lasers [36]. Since 1.55 $\mu$m lasers have smaller band-gap than 1.3 $\mu$m ones, Auger recombination rate for InGaAsP lasers operating at 1.3 $\mu$m are smaller and have the values between $2.3\pm1\times10^{-29}cm^6s^{-1}$ [1]. The value of C is also affected by the doping of the material and is bigger for doped materials. There are some differences between calculated and measured values of C. The measured Auger coefficient is usually smaller (by a factor of 3 to 5) than the theoretical values, because of various approximations and uncertainties in the band- structure parameters used in theoretical calculations.

### 3.4.2. Defect and Surface Recombination

Defects in the active region of an injection laser can be formed in several ways. In many cases they are grown in during the epitaxial growth process. Among these DLD (dark line defects), DSD (dark spot defects) can be taken into account for the high degradation of early AlGaAs lasers.

In an injection laser, the cleaved facets are surfaces

exposed to the ambient. In addition, in many index guided laser structures, the edges of the active region can be in contact with curved surfaces, which may not be a perfect lattice. A surface, in general, is a strong perturbation of the lattice, creating many dangling bonds that can absorb impurities from the ambient. Hence a high concentration of defects can occur that can act as nonradiative recombination centers. For an InP surface exposed to air, nonradiative recombination through the surface is about two orders of magnitude smaller than for GaAs, and therefore can be neglected in many InGaAsP grown on InP laser structures.

For the modeling of the semiconductor lasers, it is customary to lump defect and surface recombination and introduce a single parameter $A_{nr}$ as

$$R_{nr} = A_{nr}N \tag{3.26}$$

where $R_{nr}$ is nonradiative recombination rate ($cm^{-3}s^{-1}$), and $A_{nr}$ is the nonradiative recombination coefficient ($s^{-1}$) and is the inverse of the nonradiative lifetime $\tau_{nr}$ which is 10-15 nsec for InGaAsP lasers. Equation (3.26) can be rewritten in terms of $\tau_{nr}$ as

$$R_{nr} = \frac{N}{\tau_{nr}} \tag{3.27}$$

## 3.5. CONFINEMENT MECHANISM AND MODES IN LASER DIODES

There are two types of confinement mechanisms in semiconductor lasers. These are carrier confinement and optical

41

confinement. In order to confine carriers to the active region, band-gap of that region must be smaller than the surrounding layers
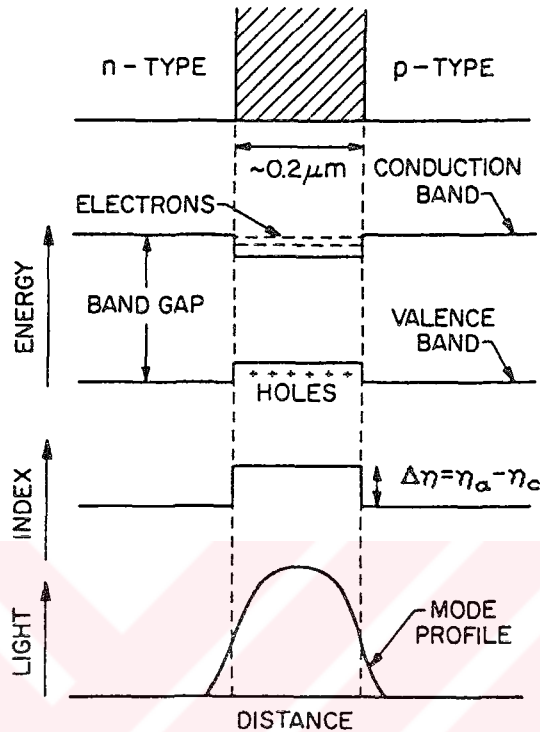


Figure 3.3 Double-heterostructure semiconductor laser configuration with simultaneous confinement of the charge carriers and optical mode to the active region (shaded area).

(e.g. cladding and waveguide). Optical confinement of photons to the active region is achieved by making refractive index of active region greater than the surrounding layers, so that the waveguidance through the more dense medium can be achievable. Double-heterostructure configuration, shown in Figure 3.3, is found to be one of the best result giving types for both carrier and optical confinement. The most important problem with this type is the lattice match between the active region and surrounding layers. InGaAsP-InP laser is the most important candidate for long-

wavelength operation since this materials can be lattice matched in a wavelength range of 0.95-1.7 $\mu$m. This wavelength shift is achieved by changing the mole fractions of quaternary solid solution $In_{1-x}Ga_xAs_yP_{1-y}$. Depending on the values of x and y, refractive index, lattice constant, and operation wavelength of the material can be changed. The relations of x-y dependence of these parameters can be given, respectively as [1]

$$\eta(y) = 3.4 + 0.256y - 0.095y^2 \qquad (x \cong 0.45y) \qquad (3.28)$$

$$a(x,y) = xy\ a(GaAs) + x(1-y)\ a(GaP)$$

$$\qquad\qquad + (1-x)y\ a(InAs) + (1-x)(1-y)\ a(InP) \qquad (3.29)$$

$$E_g(y) = 1.35 - 0.72y + 0.12y^2 \qquad (at\ 300K) \qquad (3.30)$$

where $\eta(y)$ is refractive index (dimensionless), $a(x,y)$ is lattice constant ($\mu$m), $E_g$ is band-gap energy (eV). Using well-known relation

$$E_g = \frac{hc}{\lambda} \qquad (3.31)$$

where h is the Planck's constant, c is the velocity of light in medium ($cms^{-1}$), and $\lambda$ is the wavelength which is given in microns by

$$\lambda \cong \frac{1.24}{E_g} \qquad (3.32)$$

43

For 1.3 $\mu$m operation ($E_g \cong 0.95$ eV), x=0.28 and y=0.6 lattice constant of InGaAsP is almost equal to that of InP (a=58.7 nm) which means layers are lattice-matched.

Ideally, carriers and optical mode must confine to the active region 100% but this value is not achievable in practice. Carrier leakage is responsible for reduction in carrier confinement and often referred as leakage current. Heterojunction carrier leakage is caused by diffusion and drift of electrons and holes from the edges of the active region to the cladding layers as shown in Figure 3.4. It has been shown that [1], although calculated leakage current for 1.3 $\mu$m and 1.55 $\mu$m operation at room temperature is ignorable, it achieves quite large amounts as the temperature rises.
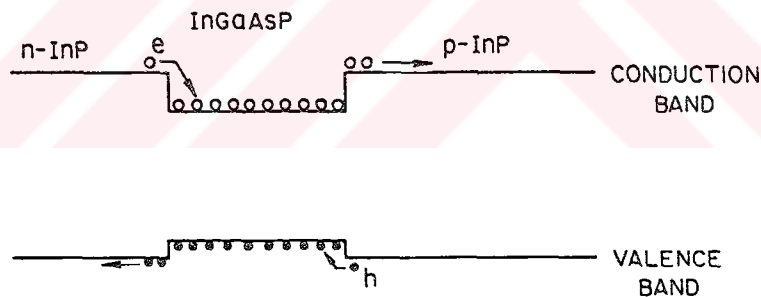


Figure 3.4 Schematic illustration of heterojunction
        leakage current.

To investigate the optical confinement mechanism, heterostructure laser is considered as symmetrical slab waveguide as shown if Figure 3.5 and Maxwell's equations are solved with boundary conditions. Although two types of transverse modes, TE and TM, are found to be solution, since facet reflectivity is found to
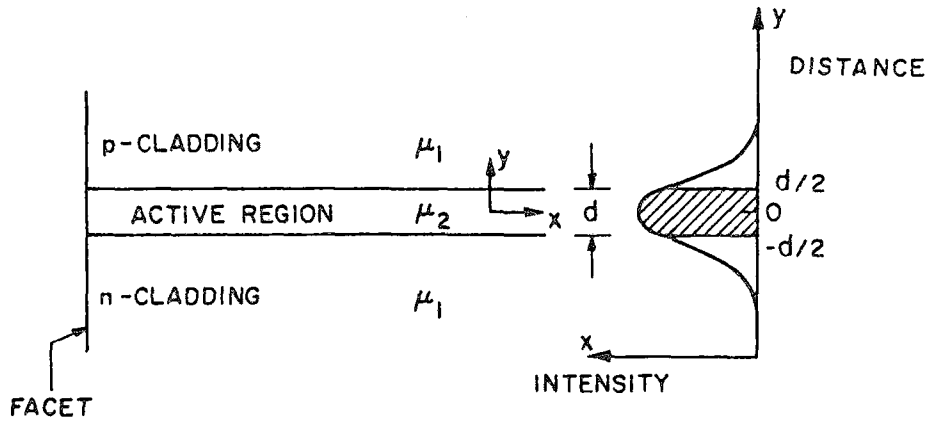
Figure 3.5 Three-layer slab-waveguide model of a semiconductor laser with $\eta_a > \eta_c$.

be higher for TE modes in Fabry-Perot type lasers, it is assumed that only TE modes will propagate [1]. The solution for single TE mode operation in transverse direction gives

$$D = \frac{2\pi}{\lambda_o} [\eta_a{}^2 - \eta_c{}^2]^{1/2} d \qquad (3.33)$$

where D is normalized waveguide thickness ($D < \pi$ corresponds to single-longitudinal mode operation), $\lambda$ is the center wavelength, d is active region thickness, and $\eta_a$ and $\eta_c$ are active region and cladding refractive indices, respectively. Transverse confinement factor $\Gamma_T$ can be found by integrating the ratio of energy in active region to the total energy and is simply [1]

$$\Gamma_T \cong \frac{D^2}{2 + D^2} \qquad (3.34)$$

Equation (3.33) gives 0.48 $\mu$m maximum active region thickness for single mode operation at 1.3 $\mu$m. For a 0.2 $\mu$m thick active region

45

laser, $\Gamma_T$ is found as 0.47 from Equations (3.33) and (3.34).

To investigate the lateral confinement mechanism, each laser structure must be considered separately since each of them has different lateral configuration. Its calculation is very similar to the calculation of transverse confinement factor for strongly index-guided lasers, such as BH (buried-heterostructure), since the boundaries of active region along lateral direction is well-defined. However, in the case of weakly index-guided lasers, such as RWG (ridge-waveguide), the boundaries along lateral direction is not well-defined and only numerical solutions to the wave equation can be obtained. In RWG laser, shown in Figure 3.6.a, the ridge induces an effective refractive index along a certain region in lateral direction and hence confines optical mode to that region as shown in Figure 3.6.b.

Overall confinement factor $\Gamma$ can be written as the product of transverse confinement factor $\Gamma_T$ and lateral confinement factor $\Gamma_L$

$$\Gamma = \Gamma_T\Gamma_L \qquad (3.35)$$

which generally takes the values in the range 0.2-0.3. The value of $\Gamma_L$ lies in the range 0.5-0.8 and can be taken as constant for RWG lasers since it cannot be calculated directly for this type. Although $\Gamma$ is taken as constant in almost all works, it is clear from Equations (3.33) and (3.34) that, it depends on waveguide thickness d. For 1.3 $\mu$m operation with typical refractive indices for active region and cladding 3.51 and 3.22, respectively, Equation (3.33) becomes

$$D \cong 6.6d \tag{3.36}$$

using equations (3.34), (3.35), and (3.36) the active region thickness dependent confinement factor can be rewritten as

$$\Gamma = \frac{(6.6d)^2}{2 + (6.6d)^2} \Gamma_L \tag{3.37}$$



(a)



(b)
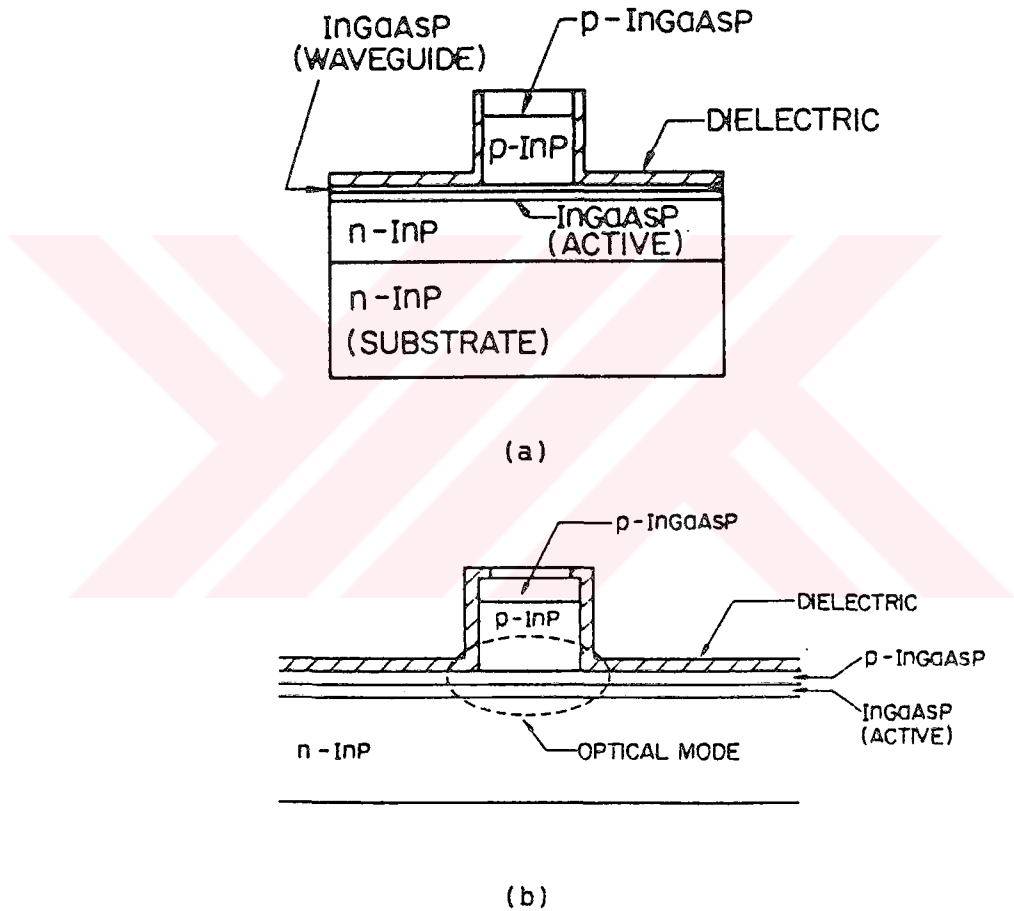
Figure 3.6 Ridge-waveguide (RWG) laser diode structure.
   (a) Schematic cross section,
   (b) optical mode in RWG laser diode.

## 3.6. LOSSES AND PHOTON LIFETIME

Fabry-Perot cavity semiconductor lasers are made of naturally cleaved facets by cutting the crystal along a certain plane and gives reflectivities about 0.32 for InGaAsP lasers. Mirror and internal losses are calculated from the threshold condition which states that optical field should reproduce itself after each round-trip under steady-state and continuous-wave (CW) operation and is given as

$$\Gamma G_{th} = \alpha_m + \alpha_{int} \tag{3.38}$$

where $G_{th}$ is the threshold gain $(cm^{-1})$, $\alpha_m$ is the mirror loss $(cm^{-1})$, and $\alpha_{int}$ is the internal loss $(cm^{-1})$. Mirror loss, in terms of laser length L and mirror reflectivities $R_1$ and $R_2$ is given by

$$\alpha_m = \frac{1}{2L} \ln(R_1 R_2)^{-1} \tag{3.39}$$

Internal loss is intrinsic and is given by

$$\alpha_{int} = \Gamma \alpha_\alpha + (1-\Gamma)\alpha_c + \alpha_{scat} \tag{3.40}$$

where $\alpha_\alpha$ is absorption loss (mainly due to free carrier absorption) in $cm^{-1}$, $\alpha_c$ is cladding absorption loss $(cm^{-1})$, and $\alpha_{scat}$ is the scattering loss at the heterojunction interfaces $(cm^{-1})$. $\alpha_{scat}$ is very small in strongly index-guided lasers, but very large in ridge-waveguide lasers and assumed to be responsible for short photon lifetimes since the diffraction losses are very large in

this type laser diodes.

Photon lifetime $\tau_p$ can be defined as the average time that a photon spends in the laser cavity before getting lost either by absorption in the active region or by leaving the cavity as light output. As the definition implies, it is inversely proportional to the mirror and intrinsic losses and given by

$$\tau_p = \frac{1}{\nu_g(\alpha_m + \alpha_{int})} \tag{3.41}$$

where $\nu_g$ is the group velocity of light in the cavity $(cms^{-1})$ and given by Equation (3.3).

It has been accepted that photon lifetime place an important role in determination of the FWHM of the output pulses such that, shorter photon lifetimes give more narrow pulses at the output. To decrease the photon lifetime losses must increase. Since internal loss $\alpha_{int}$ is mainly intrinsic, only mirror loss $\alpha_m$ can be increased to decrease photon lifetime by reducing cavity length L or mirror reflectivities $R_1$, $R_2$. Mirror reflectivities can be reduced by anti-reflection (AR) coating one or both mirrors of the laser diode. THe effects of cavity shortening and AR coating on the FWHM of the pulses has been extensively investigated in [37]. Although a short cavity laser diode is favorable for short pulse generation, it suffers from difficulties in device handling, including electrode bonding and mounting. The other way, anti-reflection coating, is very complex and requires careful electron beam operation. In addition, both of these techniques increases the threshold current of the laser diode.

49

## 3.7. COMPLETE MATHEMATICAL MODEL

In this work, a comprehensive multi-mode rate equation model of the gain-switched semiconductor laser diode is developed. Although weakly index-guided InGaAsP ridge-waveguide laser operating at 1.3 $\mu$m is considered, the model can be used to simulate the output of any direct modulated Fabry-Perot semiconductor laser operating in long-wavelength ($\lambda > 1$ $\mu$m) by changing certain parameters. Since many real lasers give multi-mode output, multi-mode rate equation model is a natural choice to explain laser's behavior.

For better approximation to the experimental results, some extra terms are included in this model. Most importants of these are gain compression, Auger recombination and nonradiative recombination. Gain and spontaneous emission are included as spectrum, since each mode experiences different gain and spontaneous emission coupled to each mode is different. In addition, some geometry dependent parameters such as, confinement factor, spontaneous emission factor and photon lifetime are taken in terms of active region dimensions of the laser diode to investigate the effect of geometry on the output of the laser diode. Moreover, carrier density dependent spontaneous radiative recombination is included to achieve more realistic results. Originality of this work arises from this extensive model which contains all of the above concepts together. As mentioned before, multi-mode rate equations are made up of one equation for the change in carrier density and a number of equations (actually this number is the number of modes oscillating) for change in the photon

50

densities of each mode. Electrons in the cavity are supplied by injection current I, and is consumed either by stimulated emission or spontaneous recombination which includes all nonradiative and radiative recombination processes. This phenomena is the description of the equation which corresponds to change in the electron density N. On the other hand equations corresponding to the change in the i-th photon density can be described as follows: Contribution to the photon density of the i-th mode comes from the optically confined parts of radiatively recombined electrons and stimulated emission as well. This photons now will either leave the cavity to give light or absorbed in the active region by several mechanisms explained in Section 3.6. In other words, they spend an average time $\tau_p$ in the cavity. The complete rate equations for electron density and photon density in i-th mode are given respectively as

$$\frac{dN}{dt} = \frac{I}{qV} - (R_{nr} + R_s + R_\alpha) - \sum_{i=-M}^{M} S_i G_i \qquad (3.42)$$

$$\frac{dS_i}{dt} = \Gamma S_i G_i - \frac{S_i}{\tau_p} - R_{ss_i} \qquad (3.43)$$

First term at the right hand-side of the Equation (3.42) is the injected electron density by current I (A) to the active region of volume V (cm$^3$) and q is the electronic charge (As). Second term includes spontaneous recombination (radiative and nonradiative) where $R_{nr}$ is the nonradiative recombination rate (cm$^{-3}$s$^{-1}$), $R_s$ is the total radiative spontaneous emission rate (cm$^{-3}$s$^{-1}$), and $R_\alpha$ is

51

the Auger recombination rate ($cm^{-3}s^{-1}$). The last term corresponds to the total stimulated emission rate, where $G_i$ is the gain of i-th mode ($s^{-1}$), $S_i$ is the photon density in i-th mode ($cm^{-3}$). M is the number of side modes and total number of modes is 2M + 1.

First term at the right hand-side of the equation (3.43) is the part of stimulated emission that confined to mode i, where $\Gamma$ is the optical confinement factor. Second term corresponds to the rate of photons in mode i leaving the cavity, and $\tau_p$ is the average lifetime of photons. The last term, $R_{ss_i}$ ($cm^{-3}s^{-1}$), is the radiative spontaneous emission that coupled to mode i.

Equation (3.42) can be rewritten using $R_{nr}$, $R_s$, $R_\alpha$, $G_i$ given by Equations (3.27), (3.17), (3.25), (3.14) as

$$\frac{dN}{dt} = \frac{I}{qV} - \left[ \frac{N}{\tau_{nr}} + (B_0 - B_1 N)N^2 + CN^3 \right]$$

$$- \sum_{i=-M}^{M} S_i \frac{g_0}{1 + \in_c \sum_{i=-M}^{M} S_i} \left\{ \frac{1}{1 + \left[ \frac{2i\delta\lambda}{\Delta\lambda_g} \right]^2} N - N_0 \right\} \qquad (3.44)$$

where N is the carrier (electron) density ($cm^{-3}$), $\tau_{nr}$ is the nonradiative recombination lifetime (s), $B_0$ ($cm^3s^{-1}$) and $B_1$ ($cm^6s^{-1}$) are radiative recombination coefficients, C is the Auger recombination coefficient ($cm^6s^{-1}$), $g_0$ is the gain constant ($cm^3s^{-1}$), $\in_c$ is gain compression parameter ($cm^3$), i is the mode number, $\delta\lambda$ is the mode separation (cm), $\Delta\lambda_g$ is the FWHM of the gain spectrum (cm), and $N_0$ is the electron transparency ($cm^{-3}$).

Similarly using $G_i$, $\tau_p$, $R_{ss_i}$ given by Equations (3.14),

52

(3.41) and (3.24) Equation (3.43) can be rewritten as

$$\frac{dS_i}{dt} = \Gamma S_i \frac{g_o}{1 + \epsilon_c \sum_{i=-M}^{M} S_i} \left\{ \frac{1}{1 + \left[\frac{2i\delta\lambda}{\Delta\lambda_g}\right]^2} N - N_o \right\}$$

$$- (B_o - B_1 N)N^2 \frac{K\Gamma\lambda_o^4}{8\pi^2\eta_a^2\eta_g\Delta\lambda_s V} \frac{1}{1 + \left[\frac{2i\delta\lambda}{\Delta\lambda_s}\right]^2}$$

$$- S_i \nu_g (\alpha_m + \alpha_{int}) \tag{3.45}$$

where $\nu_g$ is the group velocity of light in the cavity $(cms^{-1})$, $\alpha_m$ and $\alpha_{int}$ mirror loss and internal losses $(cm^{-1})$ respectively, K is the spontaneous emission enhancement factor (=1 for index-guided lasers and >1 for gain-guided lasers), $\lambda_o$ is the central mode wavelength (=1.3 $\mu$m in this work) in cms, $\eta_a$ is the refractive index of active region, $\eta_g$ is the group refractive index, and $\Delta\lambda_s$ is the FWHM of the spontaneous emission spectrum (cm).

It is important to note that Equations (3.44) and (3.45) are still not complete since the effects of laser dimensions are not directly included. Variable laser dimensions, length and active region thickness of the laser diode, directly affect volume, confinement factor, mirror loss, and indirectly affect internal losses, photon lifetime, and the peak of the spontaneous spectrum. Relations of directly affected parameters with the laser dimensions are given in previous sections. Volume of the active region changes

53

with both length and active region thickness as indicated in Equation (3.20), confinement factor changes with active region thickness as indicated in Equation (3.37), and mirror loss changes with cavity length as indicated in Equation (3.39). Equation (3.37) can be rewritten in the most general form as

$$\Gamma = \Gamma_L \frac{\left[ \dfrac{4\pi^2}{\lambda_o^{\,2}} \, [\,\eta_a^{\,2} - \eta_c^{\,2}\,]\, d^2 \right]}{2 + \left[ \dfrac{4\pi^2}{\lambda_o^{\,2}} \, [\,\eta_a^{\,2} - \eta_c^{\,2}\,]\, d^2 \right]} \qquad (3.46)$$

where $\Gamma_L$ is lateral confinement factor (assumed to be constant for ridge-waveguide lasers), and $\eta_c$ is the refractive index of cladding.

### 3.7.1. Steady-State Analysis

It is necessary to make steady-state analysis to find threshold current of the laser diode. In steady-state

$$\frac{dN}{dt} = \frac{dS_i}{dt} = 0 \qquad (3.47)$$

The steady-state threshold current of the laser diode can be determined from equation (3.42) by neglecting the stimulated emission term (since stimulated emission will be very small below threshold) as

$$I_{th} = qV \left[ \frac{N_s}{\tau_{nr}} + (B_O - B_1 N_s)N_s^2 + CN_s^3 \right] \qquad (3.50)$$

54

where $N_s$ is the steady-state electron density.

To find steady-state electron density $N_s$, the following assumptions are made:

1) The applied bias current $I_b$ is chosen greater than threshold current because if it is below threshold lasing may cease between pulses so that optical coherence between pulses is lost.

2) Above threshold, the spontaneous emission term in Equation (3.43) can be neglected.

3) Total of steady-state photon densities $\sum S_{i_s}$ is mainly determined by main mode photon density $S_{0_s}$ [29] which will be small enough so that, the term $\in_c \sum S_{i_s} \ll 1$ in Equation (3.45) can be neglected.

4) Since the main contribution to the total steady-state photon density comes from the main mode, normalized Lorentzian lineshape function in Equation (3.45) takes the value of main mode $(D_i(\lambda_0)=1)$ in steady-state (as it is shown in Figure 4.21)

Using these assumptions in Equations (3.43) and (3.45), steady-state electron density can be written as

$$N_s = \frac{1}{\Gamma g_0 \tau_p} + N_0 \tag{3.51}$$

Current I applied to the laser diode has both DC and RF components and is taken as

$$I = I_b + I_{rf}\sin(2\pi f_m t) \tag{3.52}$$

55

where $I_b$ and $I_{rf}$ are the magnitudes of the DC and RF components, respectively, $f_m$ is the modulation frequency (Hz), and t is the time (s).

Rate equations are solved by using Runge-Kutta-Fehlberg method. Standard laser diode parameters are taken for 1.3 $\mu$m InGaAsP ridge-waveguide structure laser as given in Table 3.1. Some important device parameters that affect the FWHM of pulses are taken as variables in the program. Parameters depending on the laser dimensions are included in the form that they are described in terms of laser diode dimensions.

## 3.7.2. Description of the Computer Program

After data input to the program, parameters depending on the laser dimensions such as volume, confinement factor and spontaneous emission factor are calculated. Then, steady-state analysis is made. Steady-state electron density and threshold current for given parameters are calculated. The main program that calculates the electron density and photon densities at each mode is placed in two nested loops for DC bias current and RF current. The values of N and $S_i$ are calculated at a time step of $\Delta t$. It is found that time intervals for standard parameters and no gain compression are different for gain switched laser diode output pulses to reach steady-state. When gain compression is not included pulses reach steady-state compared to the standard case. Since modulation frequency is not changed in the analysis, the results (photon densities as a function of time) are taken at the last 2 nsec of the calculation. Calculation range is chosen to be 0 to 16 nsec for

56

Table 3.1 The standard parameter values for 1.3 $\mu$m InGaAsP ridge-waveguide laser diode.

| Parameter definition and units | Symbol | Value |
|---|---|---|
| Nonradiative lifetime (s) | $\tau_{nr}$ | $10 \times 10^{-9}$ |
| Radiative recombination coefficient ($cm^3 s^{-1}$) | $B_0$ | $0.6 \times 10^{-10}$ |
| Radiative recombination coefficient ($cm^6 s^{-1}$) | $B_1$ | $1.1 \times 10^{-29}$ |
| Auger recombination coefficient ($cm^6 s^{-1}$) | $C$ | $4 \times 10^{-29}$ |
| Optical gain coefficient ($cm^2$) | $a$ | $4.2 \times 10^{-16}$ |
| Optical gain coefficient ($cm^3 s^{-1}$) | $g_0$ | $3.15 \times 10^{-6}$ |
| Electron transparency density ($cm^{-3}$) | $N_0$ | $1.1 \times 10^{18}$ |
| Gain compression parameter ($cm^3$) | $\epsilon_c$ | $3 \times 10^{-17}$ |
| Operating wavelength (cm) | $\lambda_0$ | $1.3 \times 10^{-4}$ |
| FWHM of gain spectrum (cm) | $\Delta\lambda_g$ | $32.5 \times 10^{-4}$ |
| FWHM of spontaneous emission spectrum (cm) | $\Delta\lambda_s$ | $87.8 \times 10^{-4}$ |
| Length of active region (cm) | $L$ | $200 \times 10^{-4}$ |
| Thickness of active region (cm) | $d$ | $0.2 \times 10^{-4}$ |
| Width of active region (cm) | $w$ | $5 \times 10^{-4}$ |
| Mirror reflectivities | $R_1, R_2$ | $0.32$ |
| Absorption loss ($cm^{-1}$) | $\alpha_a$ | $30$ |
| Cladding loss ($cm^{-1}$) | $\alpha_c$ | $30$ |
| Scattering loss ($cm^{-1}$) | $\alpha_{scat}$ | $45$ |
| Lateral confinement factor | $\Gamma_L$ | $0.5$ |
| Active region refractive index | $\eta_a$ | $3.51$ |
| Cladding region refractive index | $\eta_c$ | $3.22$ |
| Group refractive index | $\eta_g$ | $4$ |

all cases except $\in_c=0$ for which the range is taken as 0 to 32 nsec.
Two subroutines, for FWHM calculation and sorting the optimum pulse
durations corresponding to each RF current at a fixed DC bias
current, are used. FWHM of two peak photon densities of each mode
in gain switched laser diode are calculated and compared to each
other to ensure that steady-state is reached. Subroutine for FWHM
calculation is modified to detect multi-pulsing at the output. The
condition for multi-pulsing detection is taken as 20 dB which is
calculated as the ratio of main photon density peak to the peak of
the extra pulse. In DC analysis, results from FWHM calculation
subroutine are then sorted with corresponding RF currents for each
DC current and optimum RF current corresponding to minimum FWHM is
calculated. RF current is changed from 1 to $7I_{th}$ with a step size
of $0.1I_{th}$. DC current is changed from 0.5 to $2I_{th}$ with steps
$0.02I_{th}$.

The graphs of the computer simulation are given in Chapter 4.

# CHAPTER 4

# RESULTS OF THE MATHEMATICAL MODEL

## 4.1. INTRODUCTION

The rate equations derived in Chapter 3 are numerically solved for different DC and RF current values depending on what type of analysis is made. Although more than 20 modes exist under the gain spectrum with FWHM 32.5 nm, it is found that only 5 modes can oscillate. This is due to fact that the other modes cannot reach threshold and can be ignored in calculations for time saving.

Mainly four analysis are made throughout this work. These are:

1) to get relaxation oscillations and to see the effects of different laser parameters on the relaxation oscillation frequency and turn-on delay time,

2) to see the effects of different laser parameters on the gain switched laser diode (investigation of multi-pulsing at the laser diode output and calculation of mode suppression ratio (MSR) for each parameter),

3) to see the effects of different parameters on the FWHM of pulses obtained at constant DC and variable RF currents and power output of laser diode.

4) to see the effects of different parameters on the FWHM of pulses obtained at variable DC bias currents while RF current is optimized.

The parameters affecting the turn-on delay time, relaxation oscillation frequency, threshold current, FWHM of pulses and the output power of laser diode are investigated. These parameters are gain compression, nonradiative lifetime, radiative recombination coefficient, Auger recombination rate, gain constant, active region thickness, and laser diode length.

For simplicity in figures showing relaxation oscillations and gain switching, electron density and photon density are normalized at the output of the program for the first two analysis. Normalization factors are chosen to be $3 \times 10^{-18} cm^3$ for electron density and $5 \times 10^{-14} cm^3$ for photon density, which are quite near to the ones used in [24].

Each analysis is separately explained to give more detailed information about the results.

## 4.2. RELAXATION OSCILLATIONS

The purpose of this analysis is to observe the relaxation oscillations on the electron density and photon density, and to investigate the effects of different parameters on the relaxation oscillation frequency, turn-on delay, and threshold current.

## 4.2.1. The Effects of Different Laser Diode Parameters

## on the Frequency of Relaxation Oscillations

Relaxation oscillation frequency $f_r$ is calculated by using well-known relation given as

$$ f_r = \frac{1}{2\pi} \left\{ \frac{1}{\tau_n \tau_p} \left( \frac{I_b}{I_{th}} - 1 \right) \right\}^{1/2} \tag{4.1} $$

where $\tau_n$ is the electron lifetime defined as the average time that an electron spends in the conduction band before recombined radiatively or nonradiatively and its value is about 1-1.5 nsec. For $I_b=1.5I_{th}$ and $\tau_n=1.5$ nsec, $f_r$ is calculated from Equation (4.1) as 2.89 GHz for standard parameters and 3.45 GHz with laser diode length L=100 $\mu$m. $f_r$ is also measured for different parameters. The calculated and the measured $f_r$ values are given in Table 4.1. It is found that, the measured $f_r$ is different for all parameters. This is due to the fact that effects of all these parameters except laser diode length are neglected in derivation of Equation (4.1). Since higher relaxation oscillation frequency corresponds to shorter distance between the subsequent peaks in the photon density, it reduces the pulse duration as well. Comparison of the measured $f_r$ values for different parameters shows that maximum relaxation oscillation frequency is achieved at L=100 $\mu$m. This also indicates that this shortened cavity length will produce shorter duration optical pulses as will be seen through the following sections.

Table 4.1 Comparison of calculated and measured values of relaxation oscillation frequency $f_r$ and turn-on delay time $t_d$. Threshold current ($I_{th}$) and mode suppression ratio (MSR) for each parameter type are also given.

| Parameter type (or value) | Calcul. $f_r$ -GHz | Measur. $f_r$ -GHz | Calcul. $t_d$ -ns | Measur. $t_d$ -ns | Thr.cur. $I_{th}$ -mA | MSR -dB |
|---|---|---|---|---|---|---|
| Standard | 2.89 | 2.89 | 2.41 | 2.48 | 32.07 | 3.01 |
| $\in_c=0$ | 2.89 | 2.75 | 2.41 | 2.48 | 32.07 | 3.1 |
| $\in_c=6.7\times10^{-17}cm^3$ | 2.89 | 2.97 | 2.41 | 2.48 | 32.07 | 3.03 |
| $\tau_{nr}=15$ ns | 2.89 | 2.78 | 2.62 | 2.66 | 29.49 | 3.13 |
| $B_0=0.9\times10^{-10}cm^3s^{-1}$ | 2.89 | 3.4 | 1.81 | 1.87 | 42.66 | 2.49 |
| $C=6\times10^{-29}cm^6s^{-1}$ | 2.89 | 3.31 | 1.88 | 1.93 | 41.12 | 2.68 |
| $a=2.5\times10^{-16}cm^2$ | 2.89 | 3.31 | 1.62 | 1.70 | 65.45 | 2.3 |
| $d=0.15$ $\mu m$ | 2.89 | 3.08 | 1.89 | 1.96 | 37.59 | 2.48 |
| $L=100$ $\mu m$ | 3.45 | 3.69 | 1.86 | 1.89 | 25.7 | 10.9 |

## 4.2.2. The Effects of Different Laser Diode Parameters on the Turn-on Delay Time

Turn-on delay is defined as the time passed between the application of the input signal and occurrence of first peak in the photon densities. It is a characteristic of laser diode and indicates that stimulated emission does not occur until the carrier density has reached its threshold value $N_s$. The turn-on delay time $t_d \cong \tau_e$, where $\tau_e$ is the effective carrier recombination time given by

$$\frac{1}{\tau_\odot} = \left[\frac{1}{\tau_{nr}} + (B_O - B_1 N) + CN^2\right] \qquad (4.2)$$

If steady-state electron density is taken into account in Equation (4.2), $t_d$ can be written as

$$\frac{1}{t_d} = \left[\frac{1}{\tau_{nr}} + (B_O - B_1 N_s) + CN_s^2\right] \qquad (4.3)$$

As it is obvious from Equation (4.3), turn-on delay time is directly affected by nonradiative lifetime, radiative recombination coefficient, Auger recombination rate and indirectly affected by gain constant since steady-state electron density is related to the gain constant by Equation (3.51). Calculated values of $t_d$ from Equation (4.3), and measured values are given in Table 4.1 for comparison. It is obvious that calculated and measured values are very close which indicates that Equation (4.3) quite well describe the turn-on delay time. Minimum turn-on delay time (1.7 nsec) occurs at smaller gain constant ($a=2.5\times10^{-16} cm^2$) since $t_d$ is inversely proportional to the $N_s^2$ which increases considerably as the gain constant is decreased. However, turn-on delay is maximum (2.66 nsec) at increased nonradiative lifetime ($\tau_{nr}=15$ nsec) as it is also clear in Equation (4.3).

## 4.2.3. The Effects of Different Laser Diode Parameters on the Threshold Current

Threshold current of laser diode is directly affected by all parameters investigated in this work, except gain compression as it

is obvious from Equation (3.50). Calculated threshold current values for different parameters are given in Table 4.1. The maximum value of threshold current is calculated to be 65.45 mA for $a=2.5\times10^{-16}cm^2$ and the minimum threshold current is found to be 25.7 mA for L=100 $\mu$m. The effects of Auger recombination, Radiative recombination and active region thickness on the threshold current are also found to be significant. The importance of reducing the threshold current is due to fact that laser diode temperature rises as the applied current is increased which causes the device being damaged. Since the maximum power output of the practical laser diodes is restricted to a few tens of milliwatts. It will be seen from RF and DC graphs presented in next sections that in most of the cases FWHM of pulses are found to be decreasing as the RF or DC bias current is increased. Since RF and DC bias currents applied to the laser diode are given in terms of threshold current, a few tens of mA rise in threshold current will result in very high values of RF and DC bias current applied to the laser diode. As an illustrative example, if the minimum and maximum values of threshold currents given above are considered, the maximum RF current ($7I_{th}$) applied to the laser diode in RF and DC analysis will have the values 180 mA and 458 mA, respectively. Although the effect of Auger recombination on the threshold current is not more significant than that of active region volume and gain constant, this is due to the fact that radiative recombination coefficient B is taken as $B_O - B_1N$ in this work. As it is obvious, the effects of both $B_1$ and C are related with $N^3$ and hence $B_1$ weakens the effect of Auger recombination on the threshold current.

64

## 4.2.4. The Effect of Gain Compression on the Damping in the Relaxation Oscillations

If the injection current applied to the semiconductor laser is assumed to be a step function at time t=0, then the relaxation oscillations which occur in the photon and electron density are shown in Figure 4.1.a for applied DC bias current of $1.5I_{th}$. The same quantities are also shown in Figure 4.1.b for the case of $\epsilon_c=0$ (no gain compression). Both the electron and the photon densities oscillate and eventually settle down to their respective steady-state values. In both of the figures main mode and first side modes (i.e. $S_1$ and $S_{-1}$) are shown to oscillate. Second side modes cannot reach threshold and do not oscillate. This is due to fact that the applied current is not enough for these modes to overcome losses. The relaxation oscillation frequency calculated from Figure 4.1.a and 4.1.b are quite near to each other as shown in Table 4.1. This means that the gain compression does not so much change the frequency of the oscillations. However, the gain compression suppresses the oscillations in both the electron and the photon density as can be seen from Figure 4.1.a and Figure 4.1.b. Due to gain compression, the damping in the photon and electron density is reduced and oscillations die away quickly compared to the laser diode without gain compression. Therefore the effect of gain compression on the electron and photon densities can be thought to be equivalent to the effect of large value of $\beta_e$ [38]. Hence, the pulses produced from the gain switching of the laser diode should be different from those in a laser diode not exhibiting gain compression. Calculated and measured values of $t_d$ for both figures
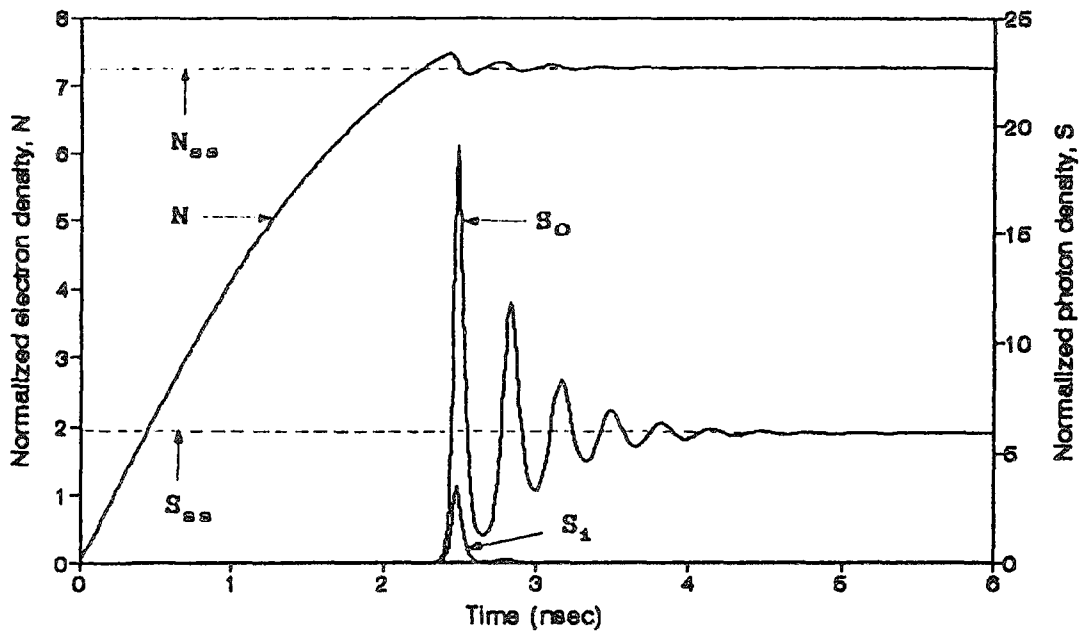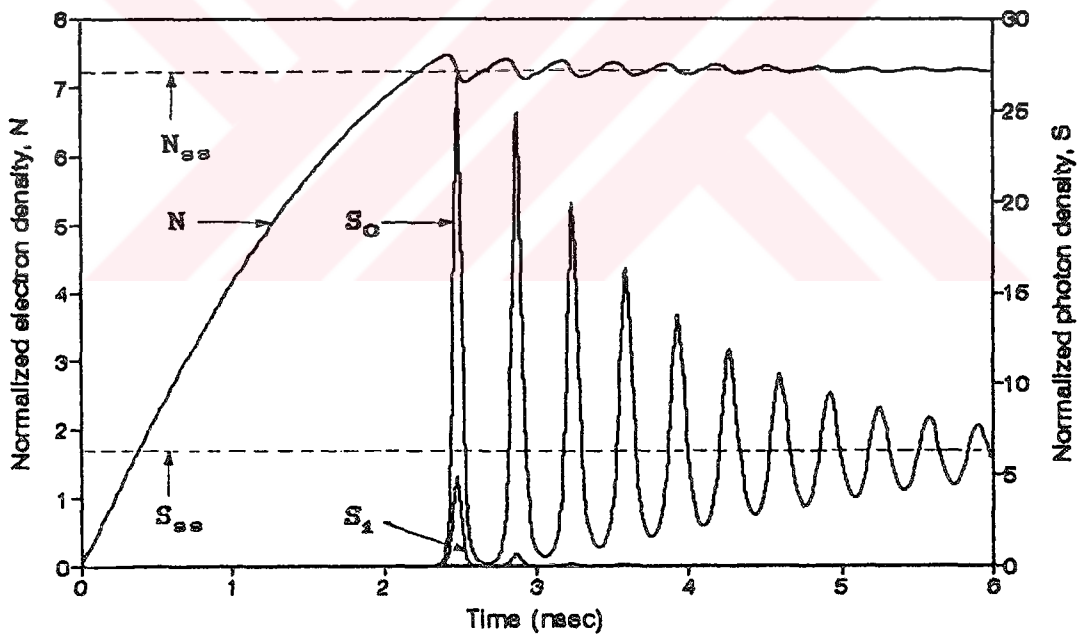
Figure 4.1 Oscillations in electron and photon densities for $I_b=1.5I_{th}$. (a) with gain compression, (b) without gain compression.

are almost the same for both cases indicating that gain compression does not affect turn-on time.

Since it is known that the most effective parameter responsible for the damping in the relaxation oscillations is the gain compression, only the graphs for standard case and no gain compression case are illustrated.

## 4.3. GAIN SWITCHING ANALYSIS

In this type of analysis both multi-mode behaviour and multi-pulsing at the output of gain switched laser diode are investigated for different parameter values.

### 4.3.1. The effects of Different Laser Diode Parameters on the Multi-Mode Behaviour of the Gain Switched Laser Diode

It is important to determine the multi-mode behaviour of the laser diode and the distribution of total output power to the modes. Therefore, it is necessary to know which parameter increases the side-mode powers and hence decreases the main-mode power. The importance of this analysis is due to the fact that multi-mode behaviour of the laser diode will affect the power distribution between the modes and hence determines the relative contribution of photon densities from different modes to the total photon density. Since the solutions of single-mode rate equations and multi-mode rate equations to find the FWHM of pulses of multi-mode operating gain switched laser diode will be compared in next sections, relative contribution of output powers of different modes to the

67

total power will give an idea about the calculated FWHM of pulses single-mode rate equations. This is due to the fact that, total photon density determines the FWHM of pulses in single-mode analysis.

An important measure to determine the relative output powers of the modes is the mode suppression ratio (MSR) which is the ratio of main mode power to the first side mode power. Mode suppression ratio (dB) is given by

$$MSR = 10 \log \left\{ \frac{P_{o_0}}{P_{o_1}} \right\} \tag{4.4}$$

Calculated MSR values for different parameters are given in Table 4.1. The output powers are measured at $I_b = 1.2 I_{th}$ and $I_{rf} = 5 I_{th}$. Comparison of calculated MSR values for different parameters given in Table 4.1 shows that, it is different for each parameter. The most effective parameter on the MSR is found to be laser diode length for which MSR is equal to 10.9 dB. Since MSR for other parameters are found to be about 3 dB, 10.9 dB is quite large compared to the other cases. This indicates that, a big portion of the total photon density comes from the main mode photon density and hence the FWHM of the pulses of total photon density will dominantly be determined by main mode photon density for L=100 $\mu$m. On the other hand, the FWHM of pulses of total photon density will tend to be determined by the first side mode photon density for the parameters having smaller MSR which are gain constant, radiative recombination coefficient, active region thickness and Auger recombination rate.

68

## 4.3.2. The Effect of Gain Compression on the Gain Switched
## Pulse Generation

Figure (4.2) shows the variation of electron density and photon density as a function of time for $I_b=1.2I_{th}$ and $I_{rf}=7I_{th}$ with standard parameters. Due to the applied RF current ($f_m=1$ GHz throughout this work), the gain of the laser diode is modulated. The electron density starts to increase as the RF current increases. Once the electron density passes its steady-state value, the photon densities increase rapidly due to the stimulated emission. The increase is very fast due to the fact that the photon lifetime is of the order of a few picoseconds. The stimulated emission rapidly depletes the electron density below its steady-state value, and hence the gain switches back. Since the applied current is also decreased below the threshold current, the electron density cannot increase above its steady-state value a second time to generate a second peak in the photon density. Hence, the generated optical pulses in this way are essentially the first peak of the relaxation oscillations in the photon density. The above description of gain switching can clearly seen from the graphs shown in Figure 4.2 and Figure 4.3. Figure 4.2.b and Figure 4.3.b are shown to clearly indicate the pulse shapes and photon densities corresponding to each mode. Unlike Figure 4.1, the photon densities corresponding to the second side modes (i.e. $S_2$ and $S_{-2}$) appear on both figures. This is because of the fact that higher RF current applied to the laser diode causes these modes to overcome threshold. The repetition rate of the optical pulses generated by gain switching is same as the repetition rate of the applied RF
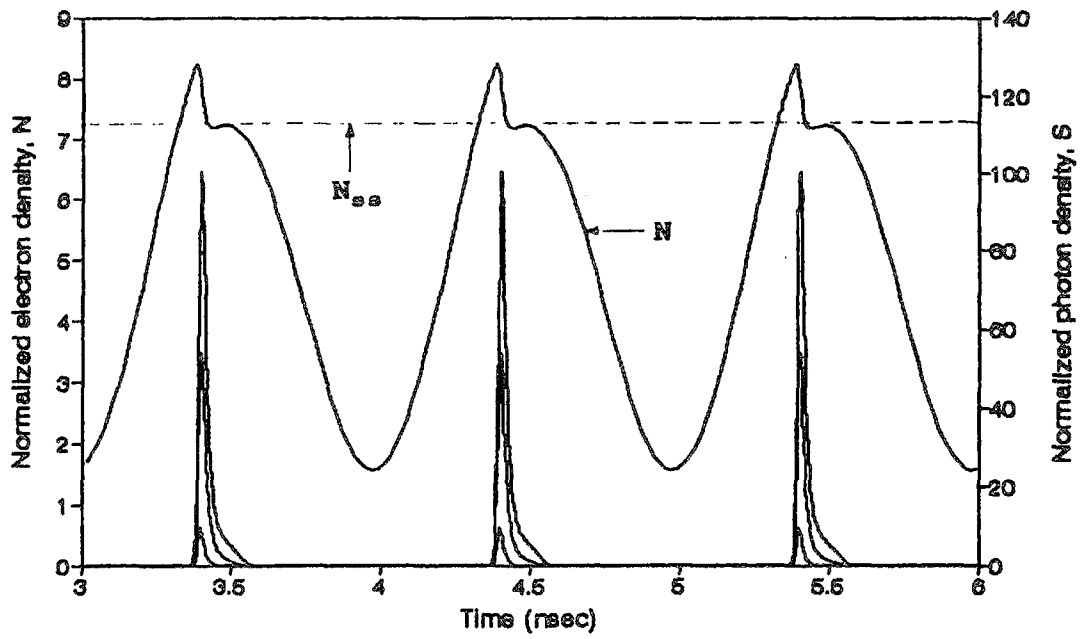
(a)
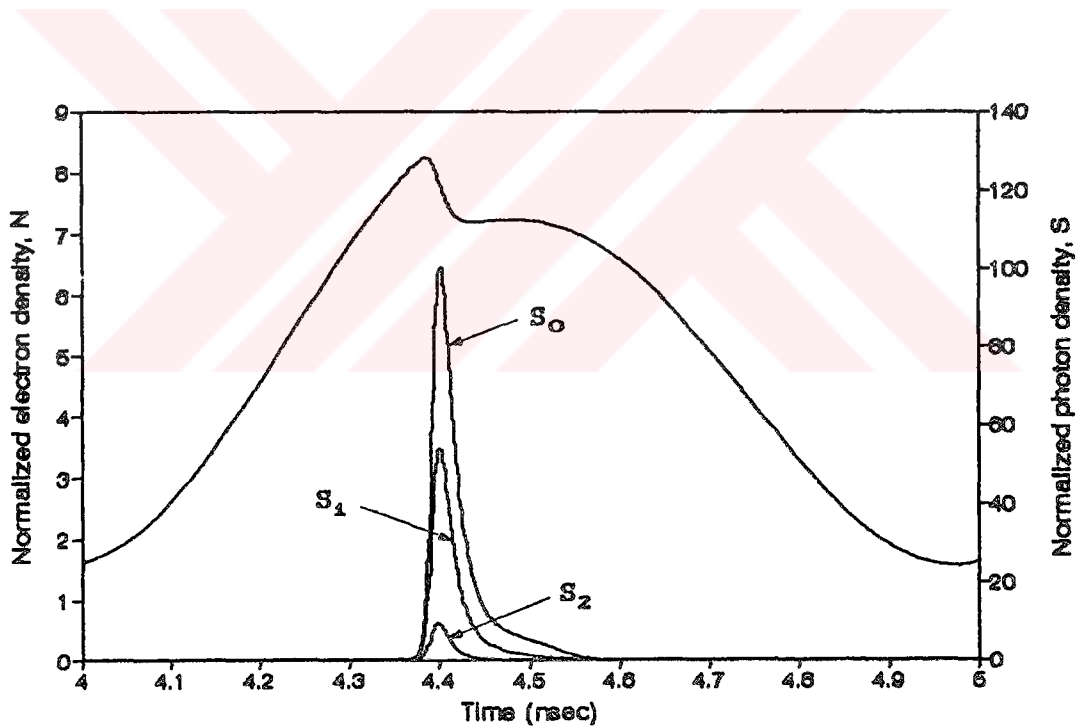


(b)

Figure 4.2 Gain switching of laser diode at $I_b=1.2I_{th}$ and $I_{rf}=7I_{th}$ with gain compression.
(a) 3 pulses of the output,
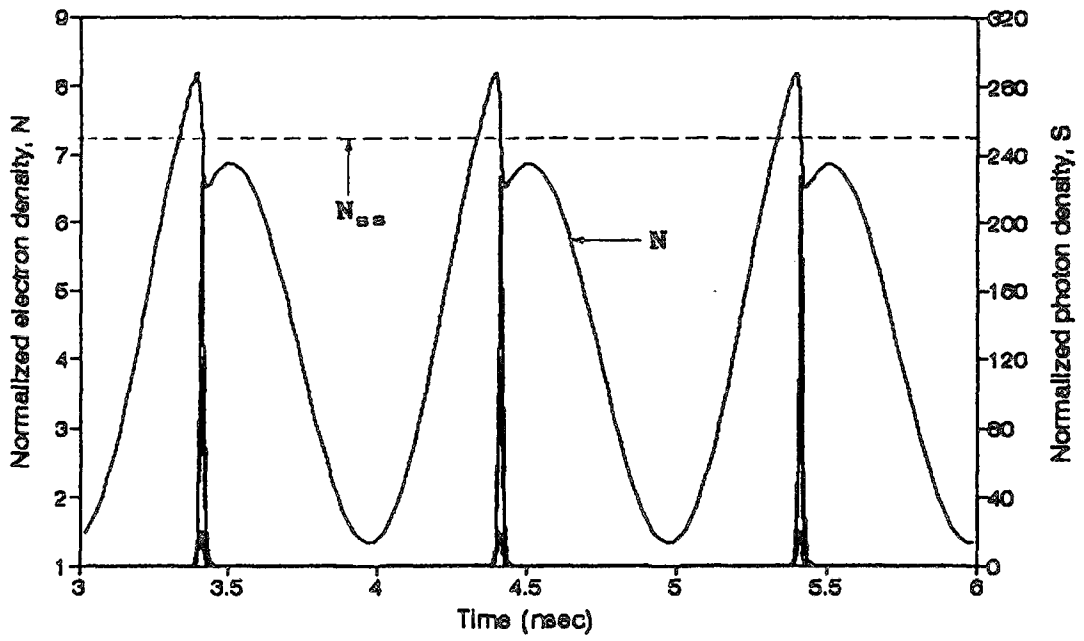(b) enlarged view of the middle pulse.

current which is 1 GHz for both standard case shown in Figure 4.2 and no gain compression case as shown in Figure 4.3.

The comparison of the optical pulses shown in Figure 4.2.b and Figure 4.3.b indicates that a laser diode exhibiting gain compression produces broader, less intense and asymmetric optical pulses, whereas the laser diode with no gain compression produces symmetrical pulses with same FWHM for all modes as will be seen on next sections.

Figure 4.3.a also indicates that electron density tries to reach threshold a second time and tend to produce a second optical pulse in the same period. This case of generation of a second pulse through a period is called as multi-pulsing and investigated in [24]. Multi-pulsing in the gain switching of the laser diode for $\epsilon_c=0$ depends on the applied current [24] and is not observed in this work because, the analysis and parameters used are different. Gain compression prevents the generation of the second pulse in the gain switching of the laser diode [24].

## 4.4. RF ANALYSIS

In this type of analysis variation of FWHM of pulses as a function of applied RF current at a fixed DC bias current of $1.2I_{th}$ for standard parameters and other parameters affecting the FWHM are investigated. FWHM of photon densities of all modes and FWHM of total photon density are given in graphs. Heavy dashed lines in all graphs (also denoted by $S_t$ as legend) denote the FWHM of total photon density and corresponds to the single-mode solution for comparison with the multi-mode solution. Although FWHM of all modes

71

(a)
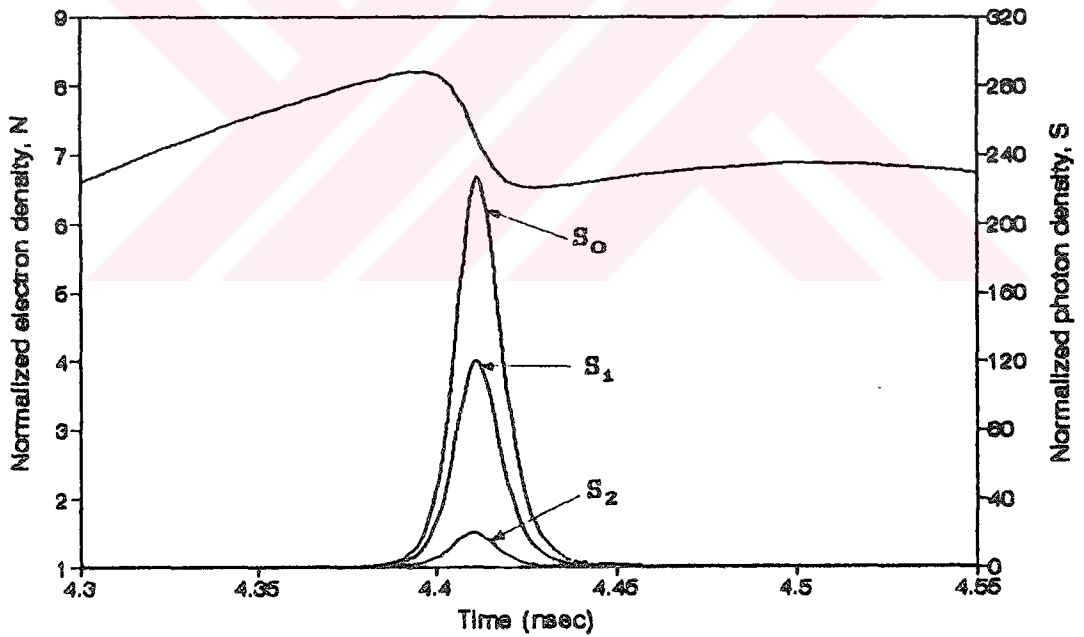


(b)

Figure 4.3 Gain switching of laser diode at $I_b=1.2I_{th}$
and $I_{rf}=7I_{th}$ without gain compression.
(a) 3 pulses of the output,
(b) enlarged view of the middle pulse.

are given in graphs, the important ones for us are the FWHM of main mode ($S_O$) and first side modes ($S_1$ and $S_{-1}$) since the photon densities of the second modes are so small that they can be ignored. RF current is changed between $1I_{th}$ and $7I_{th}$ in all graphs. The reason for the minimum value of RF current can be seen from figures indicated in this section. It is found that RF currents smaller than $1I_{th}$ do not generate short pulses. It is obvious that FWHM of pulses tend to increase as the RF current decreases. Maximum value of RF current is chosen as $7I_{th}$ as a standard. But in practice, maximum RF current applicable to the laser diode depends on the laser diode type and cooling.

Figure 4.4 shows the variation of FWHM as a function of applied RF current for standard parameters and for no gain compression case. The effect of gain compression on the pulse width can clearly be seen from Figure 4.4. In both cases, the FWHM of pulses decreases as the RF current increases. The same trend of FWHM with RF current has been indicated in [2,16,17,24]. It is important to note that for no gain compression case all modes have the same FWHM as indicated by filled triangles in Figure 4.4. For a fixed RF current $I_{rf}=I_{th}$, the pulse widths are 36 psec for $\epsilon_c=0$ and 47 psec (main mode) for the gain compression case. Minimum FWHM values corresponds to $7I_{th}$ and are, 15 psec for $\epsilon_c=0$ and 28 psec for standard parameters. FWHM of $S_O$, $S_1$ and $S_t$ are very close to each other indicating that single-mode rate equation simulation can be used in multi-mode operating lasers with same parameters used as standard parameters in this work.

Figure 4.5 shows the variation of FWHM of pulses with RF current with gain compression parameter is chosen $\epsilon_c=6.7\times10^{-17}cm^3$
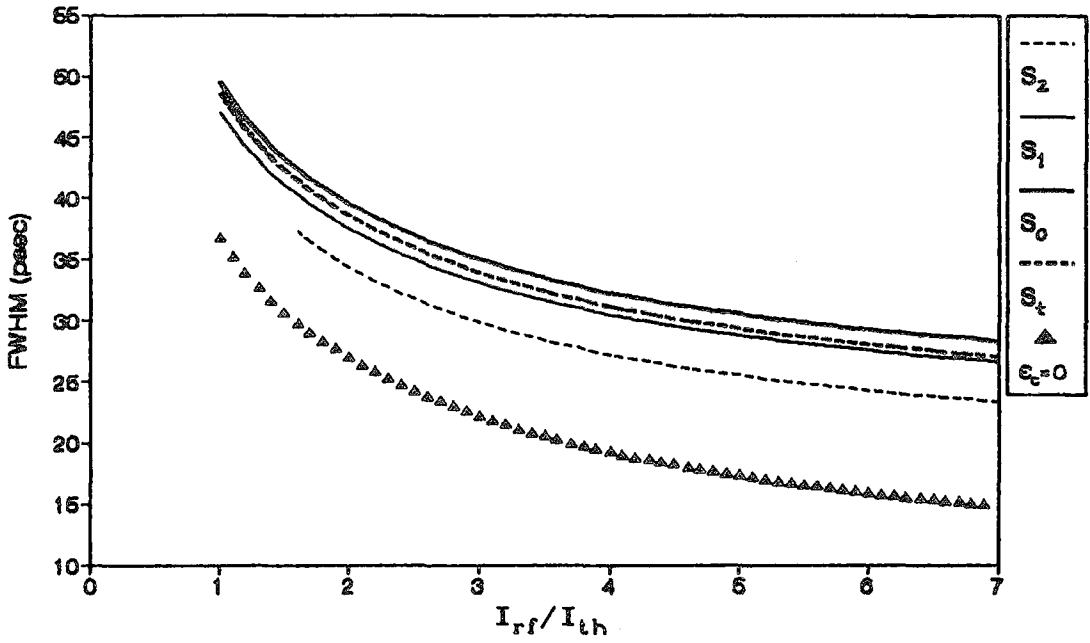
Figure 4.4 Variation of the FWHM of pulses with RF
current when $I_b = 1.2 I_{th}$ with
standard parameters values.


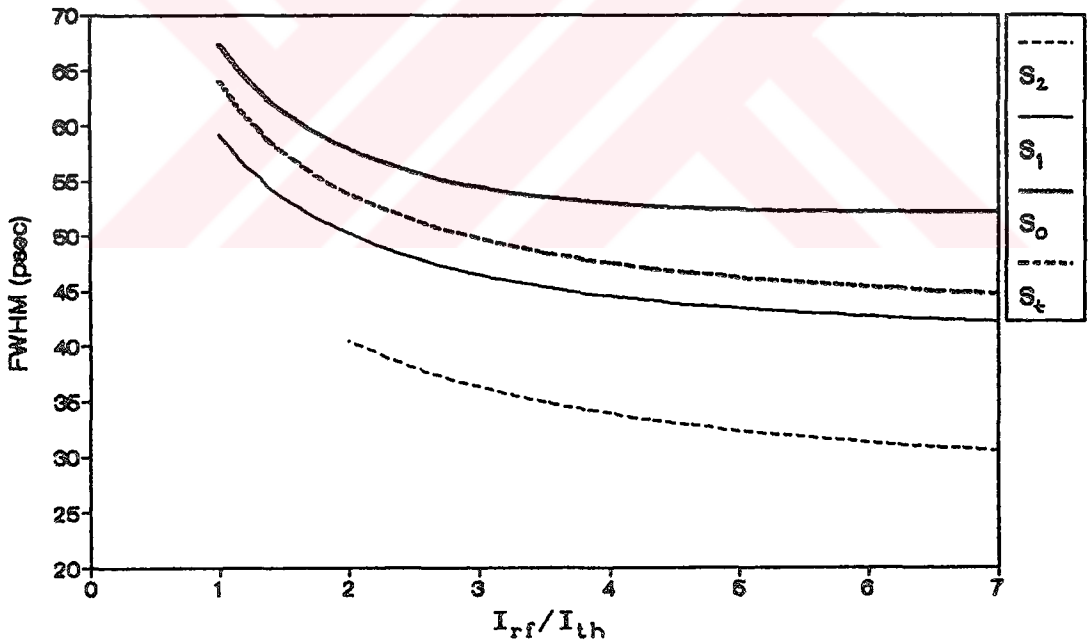
Figure 4.5 Variation of the FWHM of pulses with RF
current when $I_b = 1.2 I_{th}$ with

gain compression parameter $\epsilon_c = 6.7 \times 10^{-17} cm^3$.

[35]. Although the general trend of the graph is the same as the standard case, as the gain compression parameter is increased, pulses are broadened and FWHM of $S_t$ (single-mode solution) cannot represent the FWHM of $S_O$ and $S_1$ anymore. Maximum FWHM values occur at $I_{rf}=I_{th}$ are 67 psec for $S_O$ and 59 psec for $S_t$. As the RF current is increased, FWHM of $S_t$ gets closer to that of $S_1$ and minimum values of FWHM's are 52 psec, 45 psec and 42 psec for $S_O$, $S_t$, and $S_1$, respectively. Since a high value of gain compression parameter enhances the multi-mode behaviour of the laser diode, the photon density in first modes increases. So, contribution of photon densities first modes to the total photon density increases and this causes FWHM of $S_t$ is greatly determined by FWHM of $S_1$.

Figure 4.6 shows the variation of FWHM of photon densities as a function of RF current when $\tau_{nr}=15$ nsec. The variation is similar to the standard case but pulses are a slightly broader for $\tau_{nr}=15$ nsec. In this case maximum and minimum pulse durations occur at $I_{rf}=I_{th}$ and $I_{rf}=7I_{th}$ ,respectively as in the previous cases. Minimum FWHMs are 27 psec, 29 psec, 28 psec and maximums are 49 psec, 52 psec and 51 psec for $S_1$, $S_O$, and $S_t$, respectively. Since results for the main mode FWHM and total photon density FWHM are close to each other, single-mode solution to rate equations can be assumed to represent the behaviour of multi-mode operating laser diode with the parameters used in this calculation.

Figure 4.7 shows the effect of radiative recombination constant on the FWHM of pulses with respect to variable RF current applied to the semiconductor laser. As can be seen from the Figure 4.7 all modes can successfully oscillate for RF currents from $1I_{th}$ to $7I_{th}$. While the minimum FWHM values are the same as in the
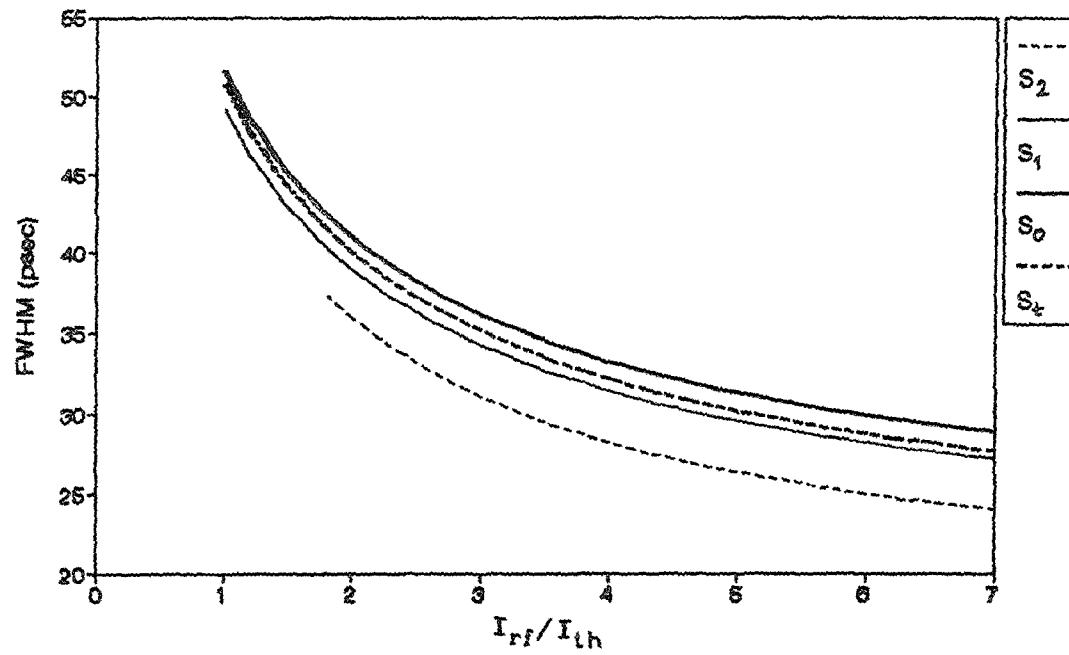
Figure 4.6 Variation of the FWHM of pulses with RF current when $I_b=1.2I_{th}$ with non-radiative lifetime $\tau_{nr}=15$ nsec.
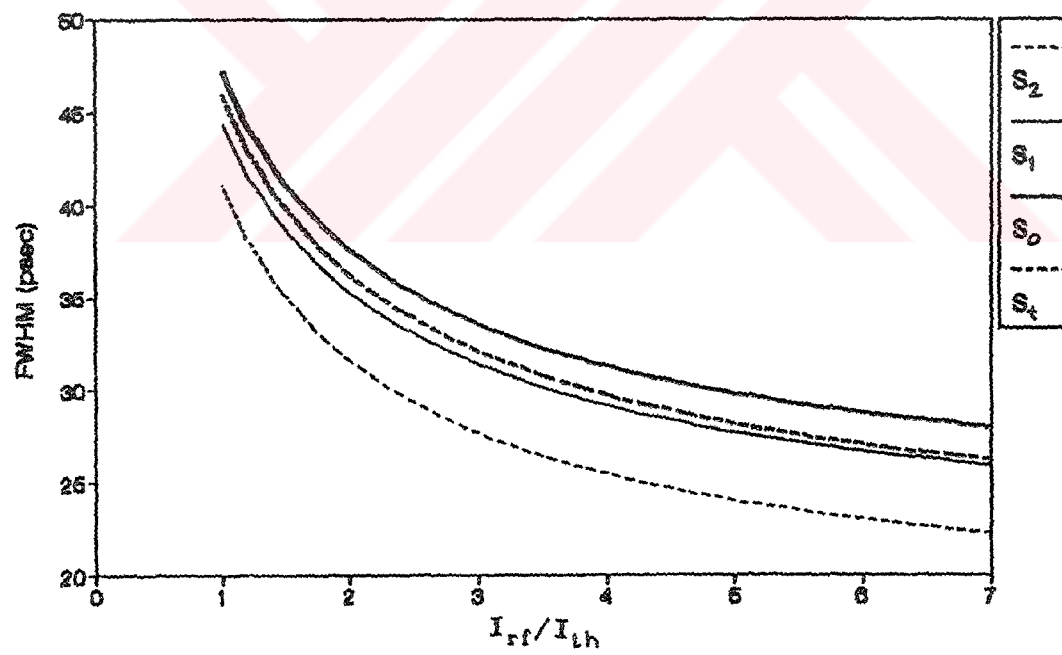


Figure 4.7 Variation of the FWHM of pulses with RF current when $I_b=1.2I_{th}$ with radiative recombination coefficient $B_o=0.9\times10^{-10}cm^3s^{-1}$.

standard case shown in Figure 4.4, the maximum values are decreased by an amount of 2 psec. There is no other effect observed on the FWHM of pulses. This indicates that there is no big difference between taking B as carrier density dependent and taking it constant as in this case. This is only true for RF analysis.

Figure 4.8 shows the effect of Auger recombination on the pulse duration for different RF currents. Auger recombination rate is increased from $4\times10^{-29}$cm$^{6}$s$^{-1}$ (standard case) to $6\times10^{-29}$cm$^{6}$s$^{-1}$. Minimum and maximum values of FWHMs of all modes are shown to decrease by an amount of 1.5-2 psec and 4-4.5 psec, respectively. But the main trend of FWHMs in this figure is same as in the standard case and other cases. The pulse durations of all modes decrease as the RF current is increased.

Figure 4.9 shows the effect of decreased gain constant a. FWHM of all modes and total photon density are increased. The increase in the maximum values of pulse durations is noticeable (9-12 psec). The change in FWHM of pulses are the same as it is in the previous cases. Pulse durations decrease as the RF current is increased. The maximum and minimum pulse durations are 51, 56, 54 psec and 35, 40, 36 psec, respectively. The difference between the FWHM of main mode and total photon density is also noticeable. This indicates that, single-mode approximation to the rate equations to investigate the output pulse duration of a multi-mode operating laser having same specifications as this case is not valid.

Figure 4.10 shows the variation of FWHM of pulses with RF current when active region thickness is reduced from 0.2 $\mu$m (standard case) to 0.15 $\mu$m. By reducing this thickness, two dimension dependent parameters are changed. These are spontaneous

77
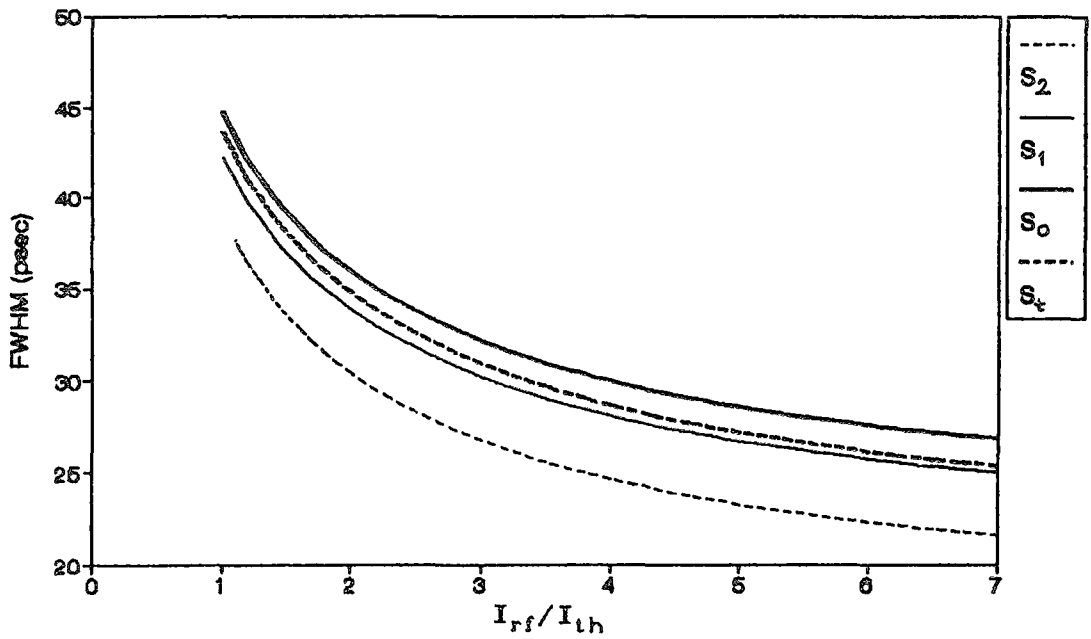
Figure 4.8 Variation of the FWHM of pulses with RF current when $I_b=1.2I_{th}$ with

Auger recombination rate $C=6\times10^{-29}cm^6s^{-1}$.


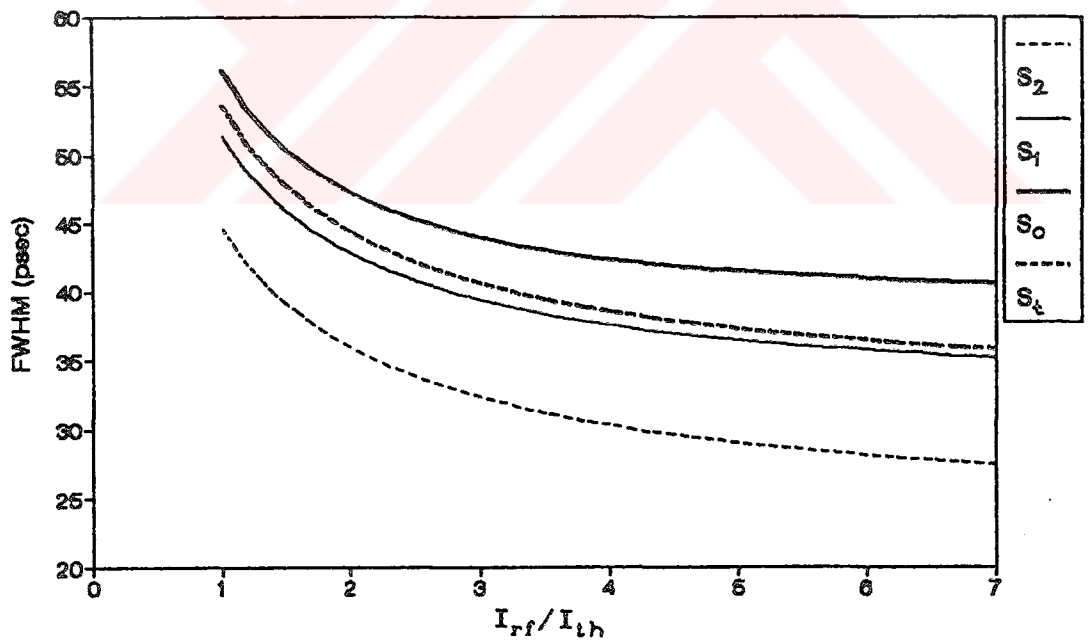
Figure 4.9 Variation of the FWHM of pulses with RF current when $I_b=1.2I_{th}$ with

gain constant $a=2.5\times10^{-16}cm^2$.

emission factor $\beta_s$ which is increased from $4.45 \times 10^{-5}$ (standard case) to $5.94 \times 10^{-5}$ and optical confinement factor $\Gamma$ which is reduced from 0.24 to 0.17. Although minimum pulse durations are the same as they are in standard case, maximum durations are decreased by an amount of 1-1.5 psec. But the figures are similar, increased RF current causes decreased pulse duration. FWHM of the main mode is close enough to that of total photon density, indicating that single-mode solutions for this multi-mode operating laser are acceptable.

· Figure 4.11 shows the variation of FWHM of pulses with RF current when laser diode length is 100 $\mu$m. By reducing cavity length from 200 $\mu$m (standard case) to 100 $\mu$m, photon lifetime is reduced from 1.01 psec to 0.71 psec and spontaneous emission factor is increased from $4.45 \times 10^{-5}$ (standard case) to $8.91 \times 10^{-5}$. As it is clear from Figure 4.11, pulse durations are shorter than the pulse durations in the standard case. In fact, the shortest pulses are obtained by cavity shortening. Since mode spacing is increased by cavity shortening ($\delta\lambda$=2.1 nm for L=100 $\mu$m while it was 1.05 nm for L=200 $\mu$m), second mode disappears in Figure 4.11. Another observation is that, the FWHM of main mode is very close to that of total photon density because main mode photon density is increased by cavity shortening and FWHM of the main mode is largely determined by the main mode photon density. The general trend of the graph is also same as the standard case, increased RF current results in shorter pulse durations obtained from laser diode. The minimum and maximum pulse durations are 19, 25, 24 psec and 35, 39,39 psec for $S_1$, $S_0$, and $S_t$, respectively.

The results of RF analysis shows that FWHM of the pulses from
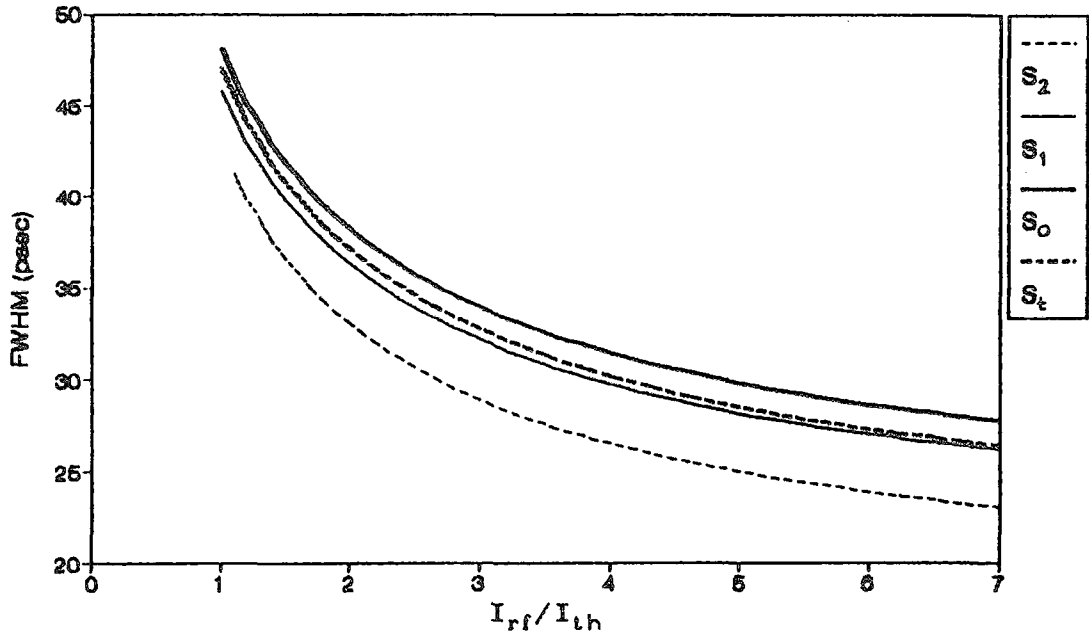
Figure 4.10 Variation of the FWHM of pulses with RF
current when $I_b=1.2I_{th}$ with
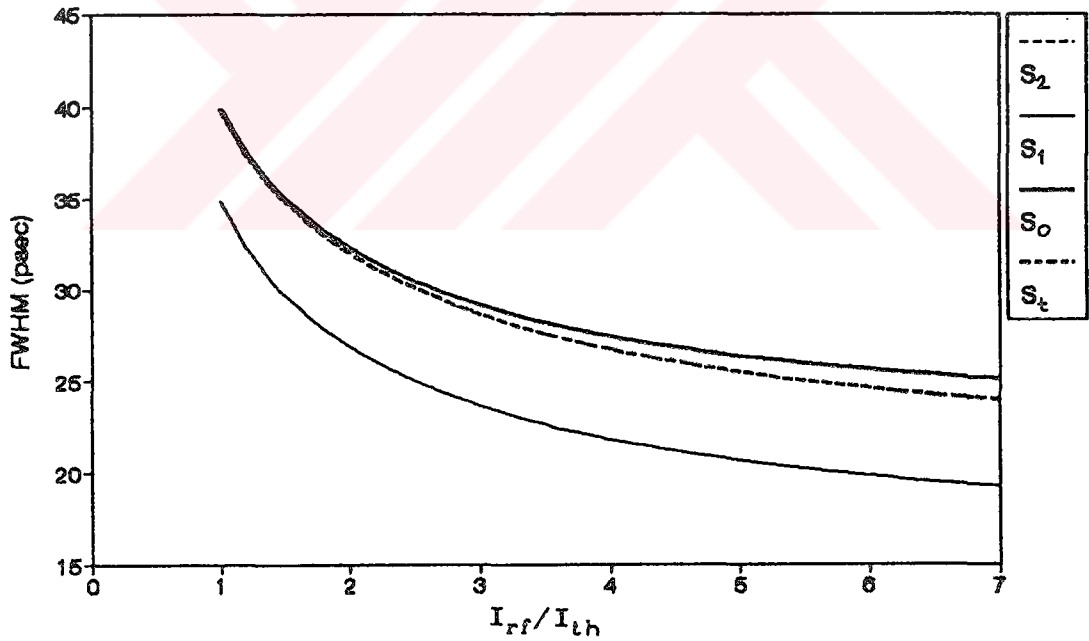active region thickness $d=0.15$ $\mu m$.



Figure 4.11 Variation of the FWHM of pulses with RF
current when $I_b=1.2I_{th}$ with
diode length $L=100$ $\mu m$.

diode laser decreases as the applied RF current is increased for all parameters. Pulse duration is largely affected by gain compression, gain constant and laser diode length. All other parameters, whose effects on the FWHM of pulses as a function of RF current are investigated, are also found to be important in determination of the pulse duration in gain switching of laser diodes.


## 4.5. DC ANALYSIS


This analysis is the most extended analysis carried out in this work, since the complete DC bias current range ($0.5I_{th}$ to $2I_{th}$) is applied to the laser diode and RF current (ranging from $1I_{th}$ to $7I_{th}$) that gives optimum pulse duration for each DC current is investigated.

Figure 4.12 shows the variation of the FWHM of pulses with DC bias current, when RF current is optimized to give minimum pulse duration , using standard parameters and $\epsilon_c=0$ (filled triangles). From Figure 4.12 it is obvious that FWHM of pulses as the DC current is increased. The difference between the no gain compression case and the standard case also increases as the DC bias current is increased. Although the decrease in the pulse durations is noticeable as the DC current increased from $0.5I_{th}$ to $1.2I_{th}$, they becomes almost insensitive to the DC bias after $1.2I_{th}$, for standard parameters. Minimum FWHM values for standard parameters occur at $I_b=2I_{th}$ are 25.3, 27.4, and 25.7 psec for $S_i$, $S_o$, and $S_t$, respectively. As shown in Figure 4.12 graph starts at $0.6I_{th}$ DC bias before which no pulses can be obtained since pulse
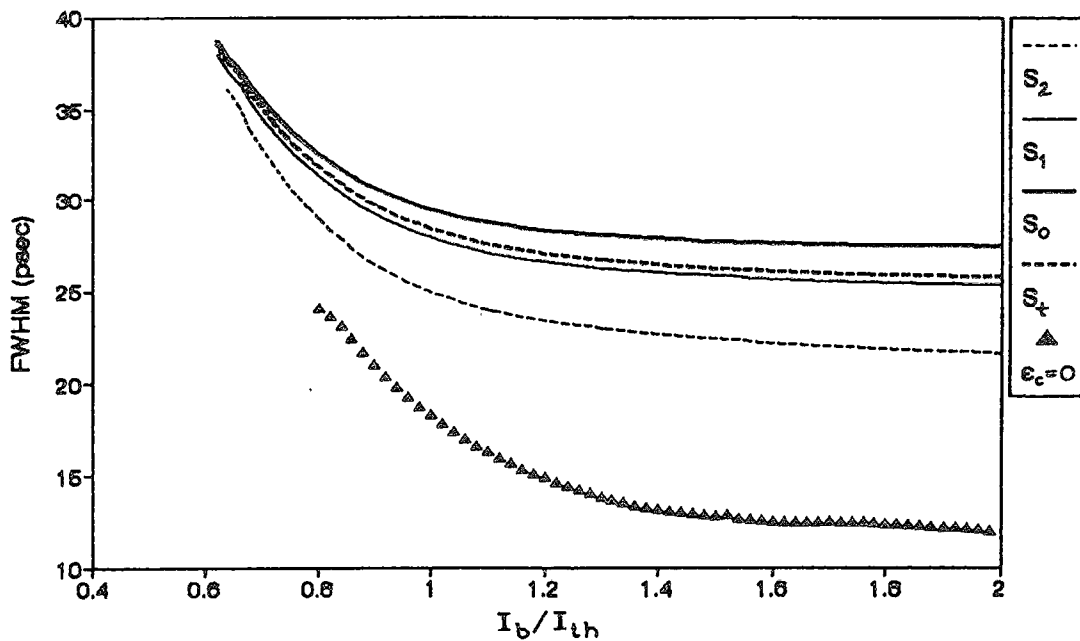
81

Figure 4.12 Variation of the FWHM of pulses with DC bias current, when RF current is optimized, using standard parameter values.
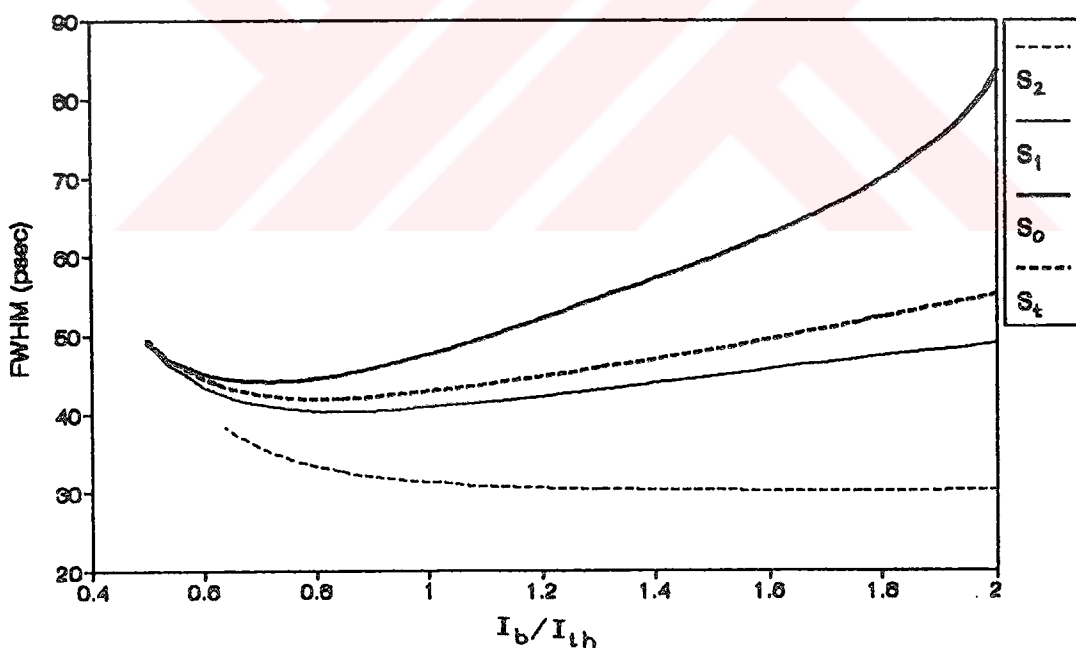


Figure 4.13 Variation of the FWHM of pulses with DC bias current, when RF current is optimized, using gain compression parameter $\epsilon_c = 6.7 \times 10^{-17} cm^3$.

solution of rate equations do not reach steady-state. The maximum of FWHM values occur at a DC bias current of $0.6I_{th}$ are 39, 38, and 38.5 psec for $S_1$, $S_o$, and $S_t$, respectively. As it is clear from the Figure 4.12 FWHM of pulses with $\epsilon_c=0$ are quite smaller than that of standard parameters. The reason behind this is explained in RF analysis for Figure 4.4. Minimum and maximum of pulse durations are 12 psec and 24 psec, respectively. In addition, all modes have the same FWHM for $\epsilon_c=0$.

Figure 4.13 shows the variation of FWHM of pulses with DC bias current for $\epsilon_c=6.7\times10^{-17}cm^3$. As it can be seen from Figure 4.13, the laser with high gain compression behaves quite different than standard case $(\epsilon_c=3\times10^{-17}cm^3)$ and no gain compression case $(\epsilon_c=0)$. FWHM of pulses are bigger than the standard case. The main trend in the graph is also different than the standard case, such that, the laser diode with high gain compression produces broader pulses as the DC bias current is increased. In fact, there is an optimum DC bias current for each photon density for which the FWHM of the pulses for this photon density is minimum. These minimum pulse durations are obtained as 40.3 psec at $0.84I_{th}$ ($S_1$), 44 psec at $0.72I_{th}$ ($S_o$), and 42 psec at $0.8I_{th}$ ($S_t$). The same type behaviour was also observed in [24] which uses the same gain compression parameter as in this case. FWHM of main mode and total photon density differ much as the DC bias current is increased. This indicates that single-mode solution of rate equations for a diode laser operating multi-mode having the same parameters used in this calculation cannot give exact FWHM values instead multi-mode analysis must be taken into account.

Figure 4.14 shows the effect of increased nonradiative

lifetime on the FWHM of pulses as a function of DC bias current. Comparison of the Figure 4.14 with Figure 4.12 (standard parameters) shows that FWHM of pulses are not affected so much with increased $\tau_{nr}$. The pulses are broadened by 0.5-1 psec which is not important compared to the FWHM of pulses. However, the results in [24] indicates that increased nonradiative lifetime causes shorter pulses at the output of the laser diode operating single mode. This contradiction arises from the different trends of FWHM of pulses as a function of DC bias current observed in this work and in [24] as mentioned in the explanation of Figure 4.12 (standard parameters).

Figure 4.15 shows the variation of FWHM of pulses as a function of DC bias when radiative lifetime is expressed as $B_O=0.9\times10^{-10}cm^3s^{-1}$. Although minimum values of FWHM of pulses are increased by an amount of 0.1-1 psec, maximum values of FWHM of pulses are decreased by approximately 2 psec compared with the standard parameter case. It is also observed that minimum of FWHM of the main mode occurs at the DC bias current of $1.34I_{th}$ and is 27.9 psec. The FWHM of total photon density is close to that of $S_1$ instead of $S_O$ indicating that main contribution to total photon density comes from $S_1$. So, single-mode solutions cannot represent the output of the laser diode multi-mode operating laser diode having the parameters used in this calculation.

Figure 4.16 shows the effect of higher Auger recombination rate on the FWHM of pulses as a function of DC bias current. Minimum values of pulse durations are decreased by an amount of 0.6-0.9 psec and maximum values are also decreased by an amount of 3-3.2 psec compared to the standard case shown in Figure 4.12. Another indication is the minimum of main mode FWHM which occurs at
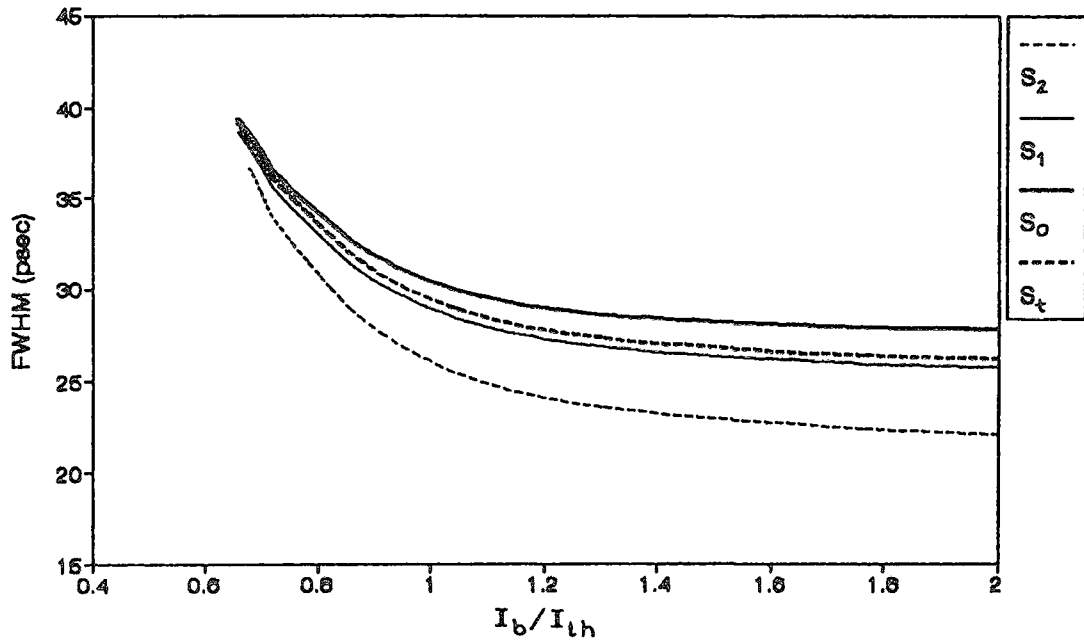
84

Figure 4.14 Variation of the FWHM of pulses with DC bias current, when RF current is optimized, using non-radiative lifetime $\tau_{nr}$=15 nsec.
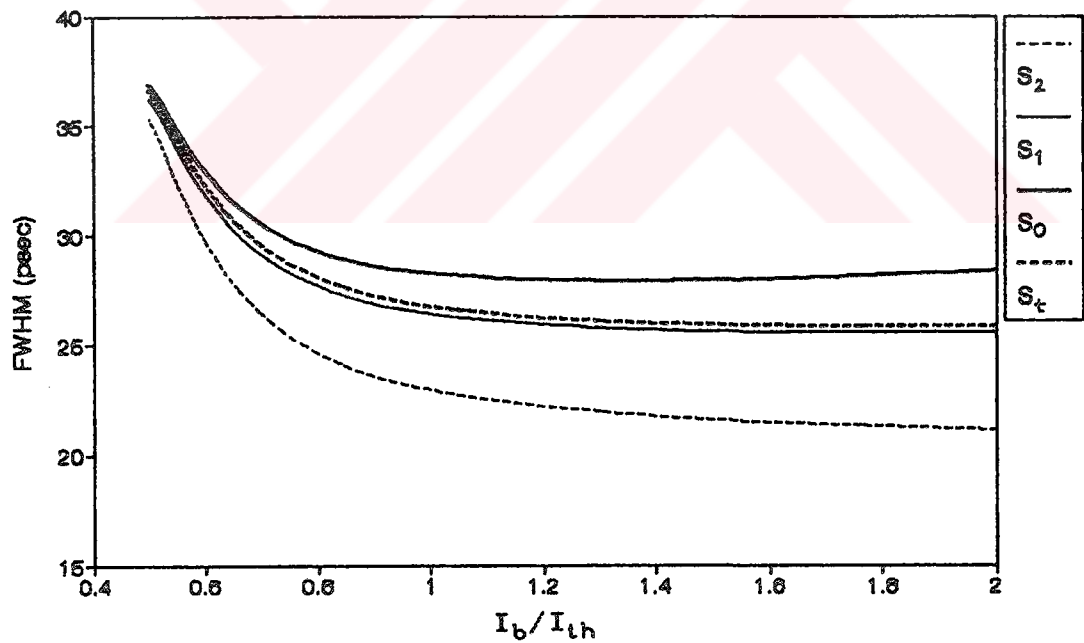


Figure 4.15 Variation of the FWHM of pulses with DC bias current, when RF current is optimized, using radiative recombination coefficient

$B_0=0.9\times10^{-10}cm^3s^{-1}$.

$1.48I_{th}$ and is 26.6 psec. The main trend of the graph is not different than the standard case except minimum of main mode FWHM mentioned above, pulses get broadened as the DC bias current increases. The difference between the FWHM of main mode and total photon density is also increased compared to standard case.

Figure 4.17 shows the effect of reduced gain constant a on the FWHM of pulses obtained as a function of DC bias current. The configuration in Figure 4.17 is quite similar to the configuration given in Figure 4.13 (for $\epsilon_c=6.7\times10^{-17}$cm$^3$) except, the FWHM values are decreased in Figure 4.17 by approximately 10 psec or more. Minimum of FWHM of pulses occur at almost the same values in both figures. For Figure 4.17, minimums are 34.3 psec at $I_b=0.84I_{th}$, 37.1 psec at $I_b=0.72I_{th}$, and 34.9 at $I_b=0.84I_{th}$ for $S_1$, $S_0$, and $S_t$, respectively. FWHM of the main mode cannot be described by the FWHM of the total photon density since they are quite different from each other. This indicates that single-mode solution of rate equations cannot give the adequate FWHM values for multi-mode operating laser considered in this analysis. Comparison of the Figure 4.17 with Figure 4.12 (standard parameter case) indicates that pulses broadened as the gain constant is decreased, as it is expected.

Figure 4.18 shows the effect of reduced active layer thickness on the FWHM of pulses as a function of DC bias current. This figure is quite similar to the Figure 4.12 (standard parameter case), in FWHM values and in general trend of FWHM values, except the maximum values of pulse durations are decreased by an amount of 1-1.3 psec compared to the solution for standard parameters. Since $\beta_s$ and $\Gamma$ are changed at the same time by reducing active region
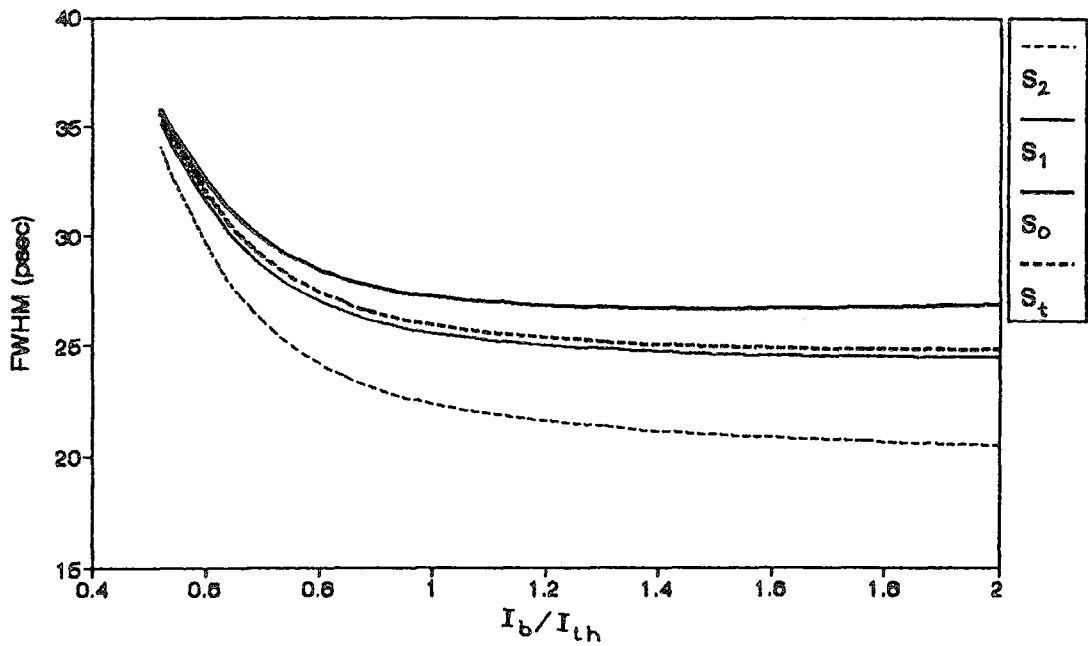
Figure 4.16 Variation of the FWHM of pulses with DC bias current, when RF current is optimized, using Auger recombination rate $C=6\times10^{-29}\mathrm{cm^6s^{-1}}$.
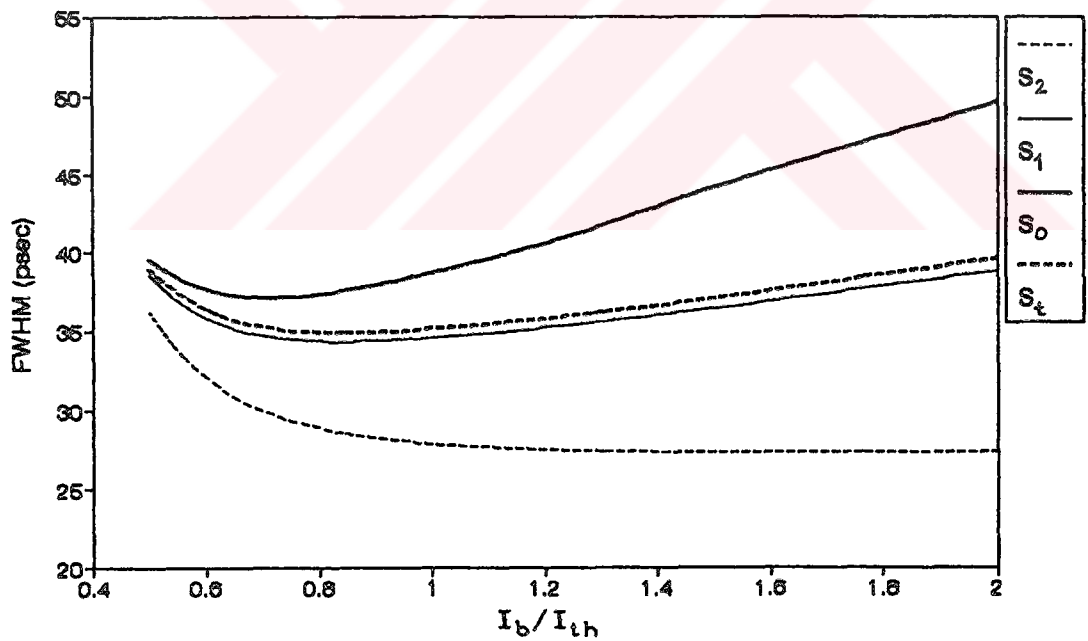


Figure 4.17 Variation of the FWHM of pulses with DC bias current, when RF current is optimized, using gain constant $a=2.5\times10^{-16}\mathrm{cm^2}$.

thickness, the effects of each of them can be considered to compensate each other. As a result, reducing active layer thickness does not affect the FWHM of pulses.

Figure 4.19 shows the variation of FWHM of pulses as a function of DC bias current when the laser diode length is 100 $\mu$m instead of 200 $\mu$m used as standard in this work. As it is obvious from Figure 4.19, pulse durations are noticeably reduced and second mode at the output is disappeared. The minimum pulse durations are 18.6 psec, 25.1 psec, and 23.8 psec for FWHM of $S_1$, $S_0$, and $S_t$, respectively. In fact, these are the shortest pulse durations obtained in this work for the laser diode that exhibits gain compression. Main mode FWHM minimum occurs at $I_b=1.28I_{th}$ and general trend of the curves shows that pulse widths are almost insensitive to the DC bias variations for the DC bias currents above $0.8I_{th}$. Since longitudinal mode spacing is inversely proportional to the cavity length, it is found using Equation (3.6) as 2.1 nm for 100 $\mu$m long laser diode whereas it was 1.05 nm for 200 $\mu$m long laser (standard parameters). Because of increased longitudinal mode spacing, second mode cannot reach threshold and first mode photon density decreases. This increases main mode photon density and FWHM of the main mode get closer to the FWHM of the total photon density. At high DC bias currents first side mode photon density increases relative to the total photon density and FWHM of the total photon density starts to be determined by both main mode and side mode photon densities. As a result, single-mode solution to the rate equations cannot explain the laser dynamics of the multi-mode operating laser diode with the specifications used in this analysis.
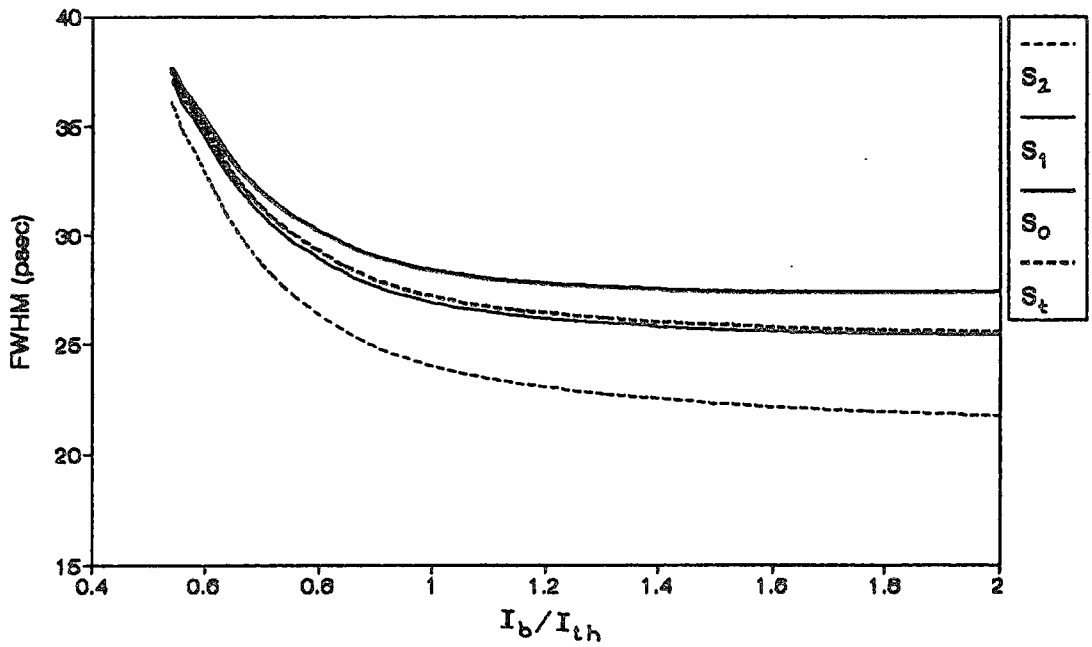
Figure 4.18 Variation of the FWHM of pulses with DC bias
current, when RF current is optimized, using
active region thickness d=0.15 $\mu$m.



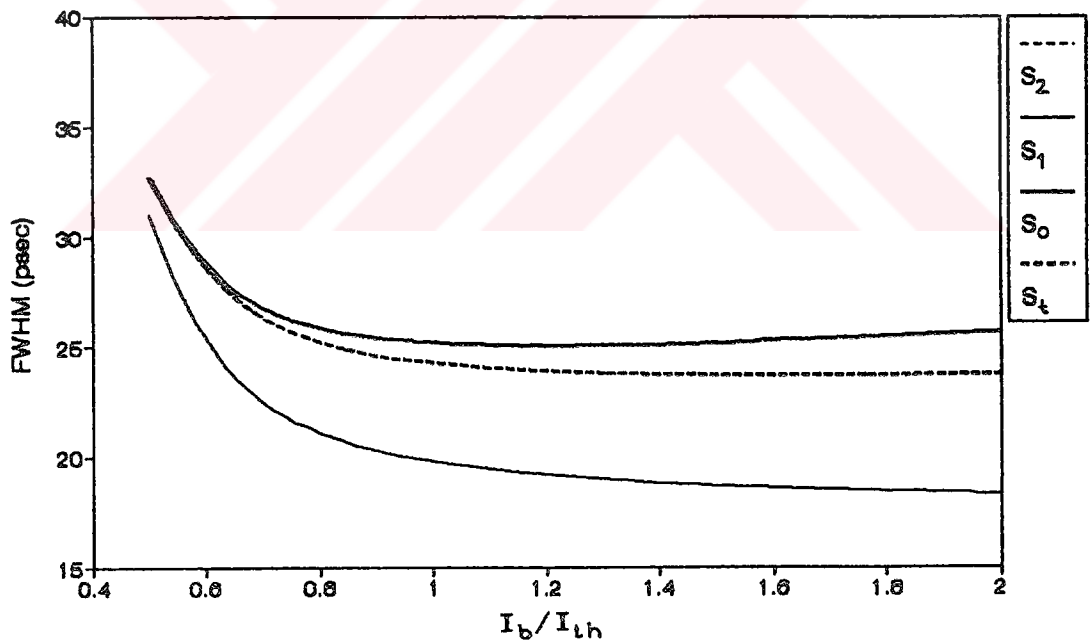Figure 4.19 Variation of the FWHM of pulses with DC bias
current, when RF current is optimized, using
diode length L=100 $\mu$m.

89

## 4.6. OUTPUT POWER OF A GAIN SWITCHED LASER DIODE

It will be better to give some explanations on the output power of modes in order to understand RF and DC behaviours of the laser diode. Since the photons in the i-th mode escape out of the laser diode cavity at a rate of $\nu_g \alpha_m$, the peak power of i-th mode emitted by each facet is related to the peak intracavity photon density in the i-th mode by the relation

$$P_{o_i} = \frac{1}{2} h\nu \nu_g \alpha_m V S_{i_p} \qquad (4.5)$$

where $P_{o_i}$ is the peak output power of the mode i emitted from each facet (eVs$^{-1}$), $h\nu$ is the energy of a photon (eV), $S_{i_p}$ is the peak photon density in mode i (cm$^{-3}$), and h is the Planck's constant (Js). After conversion of results from electronvolts to Joules, the peak power is obtained in terms of Js$^{-1}$, in other words, in terms of Watts.

Figure 4.20 shows the output peak power of each mode with RF current at $I_b = 1.2I_{th}$. Figure 4.20.a shows this variation in standard parameters case whereas Figure 4.20.b is corresponds to the case in which gain compression is not included ($\in_c = 0$). Comparison of these two figures can explain the effect of gain compression on the output power. The same effect is also be observed from Figure 4.1, since the output power is directly related with the photon density. As it is expected, the output power increases with increased RF current in both cases. This increase is almost linear when gain compression is not included as shown in Figure 4.20.b. This linearity is very useful since output
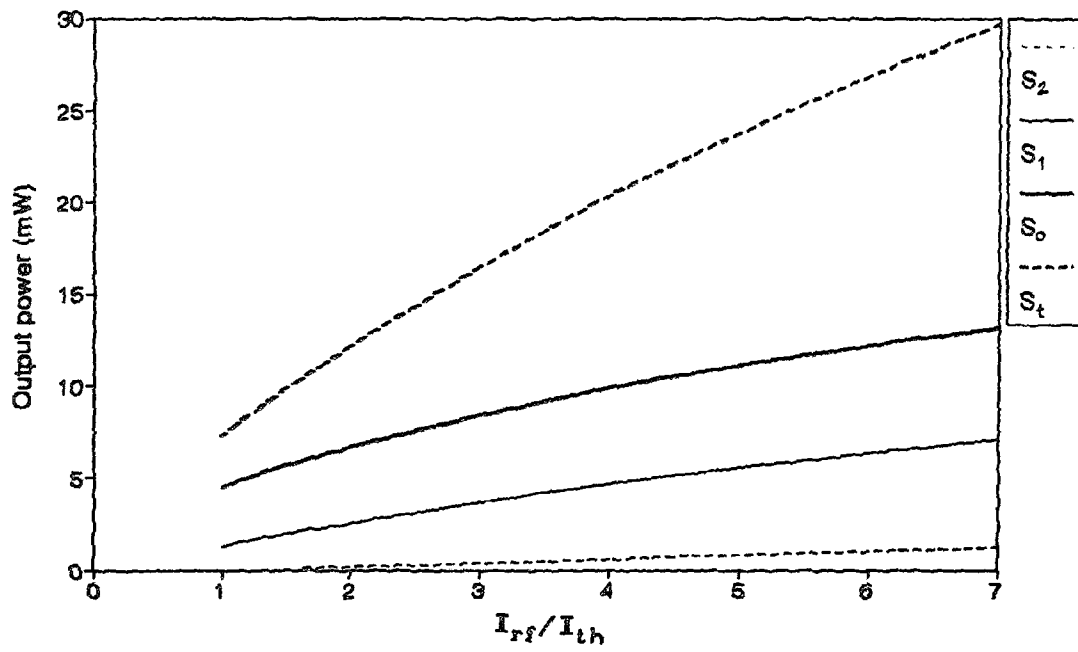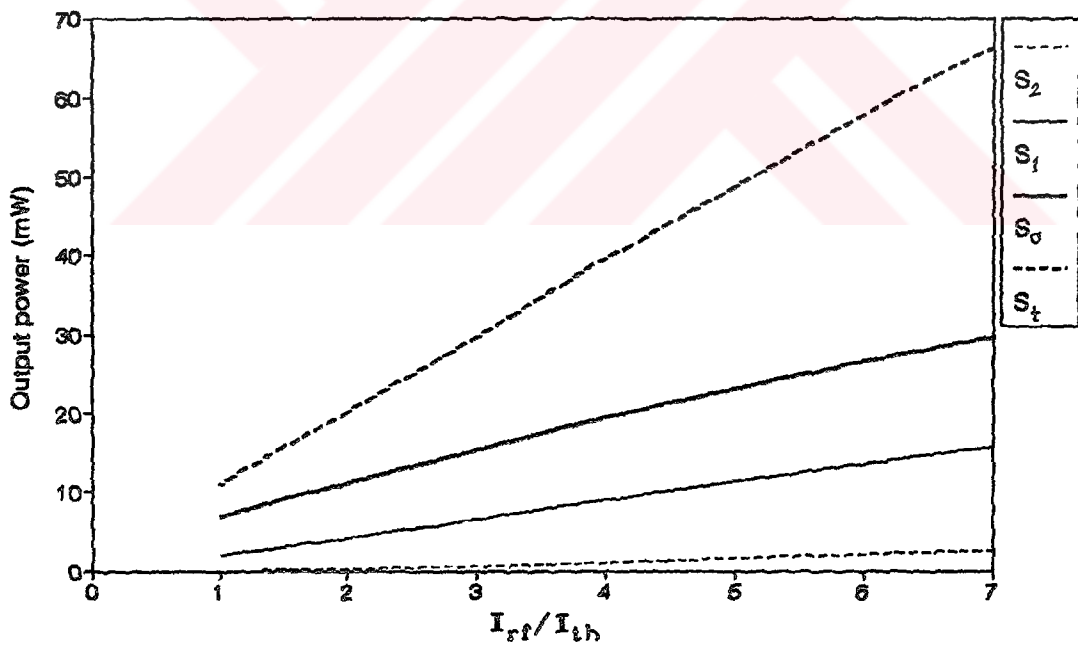
Figure 4.20 Variation of output peak power with RF
         current at $I_b = 1.2 I_{th}$ using (a) standard
         parameters, (b) $\epsilon_c = 0$ (no gain compression).

om this type of diode laser can easily be amplitude (i.e.
itensity) modulated. High power pulses are obtained at high RF
irrents at which shortest pulse durations are obtained as shown in
igure 4.4. High power pulses with short durations are the best
ies for lightwave communication systems since bandwidth and
:tenuation are directly related to the pulses used in this
/stems.

Figure 4.21 shows transient and steady-state longitudinal-
)de spectra of gain switched laser diode when $I_b=1.5I_{th}$ and $I_{rf}=0$
;ing standard parameters(as illustrated in Figure 4.1.a). The
:ansient spectrum corresponds to the first peak of relaxation
;cillations (at ~2.4 nsec) and steady-state spectrum is taken at 6
;ec after the application of the pulse. As it is clear from Figure
.21, transient mode spectrum is mainly multi-mode whereas steady-
tate spectrum is mainly composed of main mode (as it is assumed in
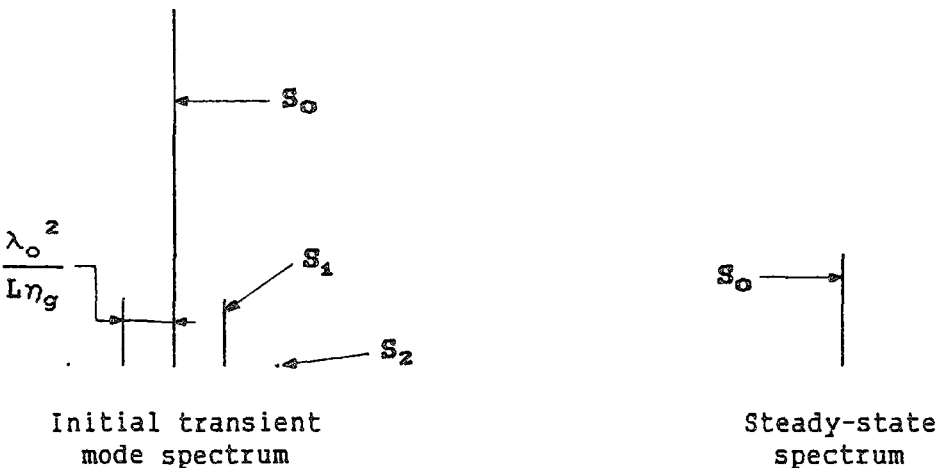iapter 3 to find the steady-state solution of rate equations).



Initial transient
mode spectrum

Steady-state
spectrum

igure 4.21 Comparison of longitudinal-mode spectra of a
gain switched laser diode under transient and
steady-state conditions.

# CHAPTER 5

## CONCLUSIONS

A theoretical model based on multi-mode rate equations which simulates the operation of gain switched multi-mode laser diode is presented. Although standard parameters are taken for 1.3 $\mu$m InGaAsP ridge-waveguide laser, the model given in this work can be used in the modelling of any gain switched semiconductor laser.

Effects of some important laser parameters on the FWHM of pulses as a function of RF and DC currents are identified. Among these gain compression, optical gain constant, Auger recombination and laser diode length are found to be the most effective ones. It is concluded that shorter optical pulses from gain switched laser diode can be obtained by laser diodes having following specifications:

1) low gain compression,

2) high optical gain,

3) short cavity length.

Gain compression and optical gain are strictly related to each other and they depend on the operating wavelength of the laser diode, structure of the laser and doping levels in the active region. A practical way of increasing optical gain is to cool the laser diode. Laser diode structure is also important since measured

gain compression is different for different structures, for example, strongly index-guided buried heterostructure (BH) lasers have smaller gain compression parameter compared to weakly index-guided ridge-waveguide (RWG) lasers. Cavity length can simply be shortened by cutting the samples during construction. Although Auger recombination is another important parameter affecting the duration of pulses, the Auger recombination rates (coefficients) taken in this work do not much affect the pulse durations. The importance of Auger recombination can be understood by comparing the laser diodes having large Auger recombination rate, for example $C=6\times10^{-29}cm^6s^{-1}$, and the ones that do not have Auger recombination [24]. To get minimum optical pulses from gain switched laser diodes, all laser diode parameters investigated in this work must be optimized.

The effects of gain constant and diode cavity length on the threshold current are found to be significant. With the same conditions given above for short pulse generation (i.e. high gain constant, low gain compression), also the threshold current can be reduced. Reducing the threshold current is very important for laser diodes as explained in Section 4.2.3.

In all calculations carried out in this work the FWHM of pulses of all modes and total photon density are found by solving multi-mode rate equations. FWHM of the total photon density calculated in this work corresponds to the solution of single-mode rate equations, which, in some works, was assumed to adequately express the laser dynamics of multi-mode operating laser diodes. The most important conclusion derived from this work is that single-mode rate equations cannot adequately describe the output of

94

multi-mode operating lasers, especially the ones with high gain compression and low optical gain.

As a future proposal, spectrum of each mode itself can be taken into account to investigate the chirping effects on the output spectrum of the gain switched laser diode. Rate equations can also be modified to include temperature effects on different laser parameters especially on the leakage current.

.

# LIST OF REFERENCES

1.  Agrawal, G.P. and Dutta, N.K., 1986. <u>Long-Wavelength</u>
    <u>Semiconductor Lasers</u>, Van Nostrand Reinhold, New York.

2.  Halley, P., 1987. <u>Fibre Optic Systems</u>, John Wiley & Sons,
    New York.

3.  Demokan, M.S., 1982. <u>Mode-Locking in Solid-State and</u>
    <u>Semiconductor Lasers</u>, Research Studies Press, Chichester.

4.  Lee, C.H., 1984. <u>Picosecond Optoelectronic Devices</u>,
    Academic Press, Inc., Orlando,Florida.

5.  Özyazıcı, M.S., 1988. <u>Ultrafast Semiconductor Lasers and</u>
    <u>Soliton Pulse Propagation</u>, Ph. D. Thesis, University
    of London, London.

6.  Eisenstein, G., Tucker, R.S., Koren, U. and Korotky, S.K.,
    1986. "Active Mode Locking Characteristics of InGaAsP Single
    Mode Fibre Composite Cavity Lasers", <u>IEEE J. Quantum</u>
    <u>Electron.</u>, Vol. QE-22, p. 142.

7.  Tucker, R.S., Korotky, S.K., Eisenstein, G., Koren, U., Stulz,
    L.W. and Veselka, J.J., 1985. "20 GHz Active Mode Locking of
    a 1.55 $\mu$m InGaAsP Lasers", <u>Electron. Lett.</u>, Vol. 21, p. 239.

8.  Ho, P.T., Glasser, L.A., Ippen, E.P. and Haus, H.A., 1978.
    "Picosecond Pulse Generation with a CW GaAlAs Laser Diode",
    <u>Appl. Phys. Lett.</u>, Vol. 33, p. 241.

9.  Olsson, A. and Tang, C.L., 1981. "Active Mode Locking of
    Linear and Ring External Cavity Semiconductor Lasers",
    <u>IEEE J. Quantum Electron.</u>, Vol. QE-17, p. 1977.

10. Demokan, M.S., 1986. "A Model of Diode Laser Actively Mode
    Locked by Gain Modulation", <u>Int. J. Electronics</u>, Vol. 60,
    p. 67.

11. Ito, H., Yokoyama, H., Murata, S. and Inaba, H., 1979.
    "Picosecond Optical Pulse Generation from a RF Modulated
    AlGaAs DH Diode Lasers", <u>Electron. Lett.</u>, Vol. 15, p. 738.

12. AuYeung, J., 1981. "Picosecond Optical Pulse Generation at
    Gigahertz Rates by Direct Modulation of a Semiconductor
    Laser", <u>Appl. Phys. Lett.</u>, Vol. 38, p. 308.

13. Totphammar, P. and Eng, S.T., 1980. "Picosecond Pulse Generation in Semiconductor Lasers using Resonance Oscillation", Electron. Lett., Vol. 16, p. 587.

14. Lin, C., Liu, P.L., Damen, T.C., Eilenberger, D.J. and Hartman, R.L., 1980. "Simple Picosecond Pulse Generation Scheme for Injection Lasers", Electron. Lett., Vol. 16, p. 600.

15. White, I.H., Gallagher, D.F.G., Osinski, M. and Bowley, D., 1985. "Direct-Streak Camera Observation of Picosecond Gain-Switched Optical Pulses from a 1.5 $\mu$m Semiconductor Laser", Electron. Lett., Vol. 21, p. 197.

16. Downey, P.M., Bowers, J.E., Tucker, R.S. and Agyekum, E., 1987. "Picosecond Dynamics of a Gain Switched InGaAsP Laser", IEEE J. Quantum Electron., Vol. QE-23, p. 1039.

17. lin, C., Burrus, C.A., Eisenstein, G., Tucker, R.S., Besomi, P. and Nelson, R.J., 1984. "11.2 GHz Picosecond Optical Pulse Generation in Gain-Switched Short-Cavity InGaAsP Injection Lasers by High-Frequency Direct Modulation", Electron. Lett., Vol. 20, p. 238.

18. Onodera, N., Ito, H. and Inaba, H., 1984. "Fourier-Transform Limited, Single-Mode Picosesond Optical Pulse Generation by a Distributed Feedback InGaAsP Diode Laser", Appl. Phys. Lett., Vol. 45, p. 843.

19. Tarucha, S. and Otsuka, K., 1981. "Response of Semiconductor Laser to Deep Sinusoidal Injection Current Modulation", IEEE J. Quantum Electron., Vol. QE-17, p. 810.

20. Ito, H., Yokoyama, H., Murata, S. and Inaba H., 1981. "Generation of Picosecond Optical Pulses with Highly RF modulated AlGaAs DH Laser", IEEE J. Quantum Electron., Vol. QE-17, p. 663.

21. van der Ziel, J.P. and Logan, R.A., 1982. "Generation of Short Optical Pulses in Semiconductor Lasers by Combined DC and Microwave Current Injection", IEEE J. Quantum Electron., Vol. QE-18, p. 1340.

22. Onodera, N., Ito, H. and Inaba, H., 1985. "Generation and Control of Bandwidth-Limited, Single-Mode Picosecond Optical Pulses by Strong RF Modulation of a Distributed Feedback InGaAsP Diode Laser", IEEE J. Quantum Electron., Vol. QE-21, p. 568.

23. Onodera, N., Ito, H. and Inaba, H., 1982. "High-Peak-Power Picosecond Optical Pulse Generation from Highly RF-Modulated InGaAsP DH Diode Laser", Electron. Lett., Vol. 18, p. 811.

24. Özyazıcı, M.S. and Demokan, M.S., 1990. "Gain-Switched Pulse Generation from a 1.55 $\mu$m InGaAsP Laser", Int. J. Optoelectronics, Vol. 5, p. 7.

25. Aspin, G.J. and Carrol, J.E., 1981. "The Effect of Cavity Length on Picosecond Pulse Generation with Highly RF modulated AlGaAs Double Heterostructure Lasers", Appl. Phys. Lett., Vol. 39, p. 860.

26. Osinski, M. and Adams, M.J., 1985. "Picosecond Pulse Analysis of Gain Switched 1.55 $\mu$m InGaAsP Lasers", IEEE J. Quantum Electron., Vol. QE-21, p. 1929.

27. Paoli, T., 1981. "Optical Response of a Stripe-Geometry Junction Laser to Sinusoidal Current Modulation at 1.2 GHz", IEEE J. Quantum Electron., Vol. QE-17, p. 675.

28. Cartledge, J.C. and Elrefaie, A.F., 1990. "Threshold Gain Difference Requirements for Nearly Single-Longitudinal-Mode Lasers", J. Lightwave Tech., Vol. 8, p. 704.

29. Herre, P.J. and Barabas, U., 1989. "Mode Switching of Fabry-Perot Laser Diodes", IEEE J. Quantum Electron., Vol. QE-25, p. 1794.

30. Morton, P.A., Ormondroyd, R.F., Bowers, J.E. and Demokan, M.S., 1989. "Large-Signal Harmonic and Intermodulation Distortions in Wide-Bandwidth GaInAsP Semiconductor Lasers", IEEE J. Quantum Electron., Vol. QE-25, p. 1559.

31. Hjelme, D.G. and Mickelson, A.R., 1989. "Gain Nonlinearities Due to Carrier Density Dependent Dispersion in Semiconductor Lasers", IEEE J. Quantum Electron., Vol. QE-25, p. 1625.

32. Koch, T.L. and Linke, R.A., 1986. "Effect of Nonlinear Gain Reduction on Semiconductor Laser Wavelength Chirping", Appl. Phys. Lett., Vol. 48, p. 613.

33. Agrawal, G.P. and Shen, T.M., 1986. "Importance of Rapid Damping of Relaxation Oscillations for High Performance Optical Communication Systems", Electron. Lett., Vol. 22, p. 1087.

34. Tucker, R.S. and Kaminow, I.V., 1984. "High-Frequency Characteristics of Directly Modulated InGaAsP Ridge Waveguide and Buried Heterostructure Lasers", J. Lightwave Tech., Vol. 2, p. 385.

35. Byrne, D.M. and Keating, B.A., 1989. "A Laser Diode Model Based on Temperature Dependent Rate Equations", IEEE Photon. Tech. Lett., Vol. 1, p. 356.

36. Lin, C., 1989. Optoelectronic Technology and Lightwave Communication Systems, Van Nostrand Reinhold, New York.

37.  Liu, H., Fukozawa, M., Kawai, Y. and Kamiya, T.,  1989. "Gain-Switched Picosecond Pulse (<10 ps) Generation from 1.3 $\mu$m InGaAsP Laser Diodes", <u>IEEE J. Quantum Electron.</u>, Vol. QE-25, p. 1417.

38.  Boers, P.M. and Vloadingerbroek, M.T., 1975. "Dynamic Behaviour of Semiconductor Lasers", <u>Electron. Lett.</u>, Vol. 11, p. 206.